Plant Communications
Research article

CellPress
Partner Journal

Temperature changes in the root ecosystem affect plant functionality

Mary Paz González-García[1,2,5], Carlos M. Conesa[1,5], Alberto Lozano-Enguita[1], Victoria Baca-González[1], Bárbara Simancas[1], Sara Navarro-Neila[1], María Sánchez-Bermúdez[1], Isai Salas-González[3], Elena Caro[1,2], Gabriel Castrillo[4] and Juan C. del Pozo[1,*]

[1]Centro de Biotecnología y Genómica de Plantas (UPM-INIA/CSIC), Universidad Politécnica de Madrid (UPM) - Instituto Nacional de Investigación y Tecnología Agraria y Alimentaria-CSIC (INIA/CSIC), Campus Montegancedo, 28223 Pozuelo de Alarcón (Madrid), Spain

[2]Departamento de Biotecnología-Biología Vegetal, Escuela Técnica Superior de Ingeniería Agronómica, Alimentaria y de Biosistemas, Universidad Politécnica de Madrid (UPM), 28040 Madrid, Spain

[3]Undergraduate Program in Genomic Sciences, Center for Genomics Sciences, Universidad Nacional Autonóma de México, Av. Universidad s/n. Col. Chamilpa, Cuernavaca 62210, Morelos, México

[4]Future Food Beacon of Excellence & School of Biosciences, University of Nottingham, Sutton Bonington, UK

[5]These authors contributed equally to this article.

***Correspondence: Juan C. del Pozo (pozo@inia.csic.es)**

https://doi.org/10.1016/j.xplc.2022.100514

ABSTRACT

Climate change is increasing the frequency of extreme heat events that aggravate its negative impact on plant development and agricultural yield. Most experiments designed to study plant adaption to heat stress apply homogeneous high temperatures to both shoot and root. However, this treatment does not mimic the conditions in natural fields, where roots grow in a dark environment with a descending temperature gradient. Excessively high temperatures severely decrease cell division in the root meristem, compromising root growth, while increasing the division of quiescent center cells, likely in an attempt to maintain the stem cell niche under such harsh conditions. Here, we engineered the TGRooZ, a device that generates a temperature gradient for *in vitro* or greenhouse growth assays. The root systems of plants exposed to high shoot temperatures but cultivated in the TGRooZ grow efficiently and maintain their functionality to sustain proper shoot growth and development. Furthermore, gene expression and rhizosphere or root microbiome composition are significantly less affected in TGRooZ-grown roots than in high-temperature-grown roots, correlating with higher root functionality. Our data indicate that use of the TGRooZ in heat-stress studies can improve our knowledge of plant response to high temperatures, demonstrating its applicability from laboratory studies to the field.

Key words: heat stress, root, temperature gradient, nutrition, gene expression, microbiome

González-García M.P., Conesa C.M., Lozano-Enguita A., Baca-González V., Simancas B., Navarro-Neila S., Sánchez-Bermúdez M., Salas-González I., Caro E., Castrillo G., and del Pozo J.C. (2023). Temperature changes in the root ecosystem affect plant functionality. Plant Comm. **4**, 100514.

INTRODUCTION

High temperature is an adverse condition that enormously impacts plant growth and fitness (Bhattacharya, 2019). Nowadays, climate change is leading to more frequent high-temperature extremes, such as heat waves, that aggravate the negative impact of heat on plant development and agricultural yield (Gray and Brady, 2016; Miller et al., 2021). In comparison with shoot responses, root responses to high temperatures have been understudied, and the majority of studies have focused on the response to warming, which induced thermomorphogenesis responses, rather than heat stress (Nagel et al., 2009; Bellstaedt et al., 2019; Gaillochet et al., 2020; Lee et al., 2021b; Ai et al., 2022). However, there is an increasing interest in deciphering the role of roots in plant adaptation to heat stress (Huang et al., 2012; Calleja-Cabrera et al., 2020; Tiwari et al., 2022), driven primarily by general concerns about how climate change might affect

Published by the Plant Communications Shanghai Editorial Office in association with Cell Press, an imprint of Elsevier Inc., on behalf of CSPB and CEMPS, CAS.

crop production in agricultural systems (Fahad et al., 2017). Heat stress causes significant damage to proteins, disturbing their synthesis and folding, changing the activity of enzymes, and damaging membranes and cellular structures by massive oxidation (Hasanuzzaman et al., 2013). To cope with these heat-associated challenges and ensure plant fitness, plants have evolved several adaptive strategies that involve, among other responses, gene expression changes, metabolic adjustments, and modifications of morphological structures and organs (Zhao et al., 2020). High temperatures significantly alter gene expression and protein accumulation in soybean (Valdés-López et al., 2016), Arabidopsis (Bellstaedt et al., 2019; Gaillochet et al., 2020; Sriden and Charoensawan, 2022), and *Agrostis* grass species (Xu et al., 2008), among others. They also affect cell division and differentiation, reducing plant growth and development (Qi and Zhang, 2020; Liu et al., 2022). It should be noted that the majority of studies carried out to understand shoot and/or root responses to heat or warming have grown whole plants (shoots and roots) at homogeneous high temperatures and, in some cases, have heated detached shoots and roots (Heckathorn et al., 2013; Valdés-López et al., 2016; Chen and Li, 2017; Estravis-Barcala et al., 2021). However, waves of high atmospheric temperature have different effects on shoots than on roots. Because of soil geothermal properties, a decreasing temperature gradient is formed from the topsoil to deeper layers (Lynch et al., 2012), preventing overwarming of the root system and likely contributing to the maintenance of its functionality and growth (Michaletz et al., 2015).

Root system architecture (RSA), defined as the three-dimensional organization of roots in the soil, plays an essential role in water and nutrient absorption and communication with microbiota (de la Fuente Cantó et al., 2020), processes that are affected by soil temperature changes (Giri et al., 2017; Hatfield and Prueger, 2015; Onwuka, 2018; Sabri et al., 2018). RSA changes in response to heat have a genetic basis that may differ between species that have adapted to different optimum temperatures for root growth and lateral root production (Zhang et al., 2015; Gray and Brady, 2016). Depending on the species, a temperature increase has been shown to promote (Lahti et al., 2005) or inhibit (Larkindale et al., 2005; Takahashi et al., 2019) root growth.

To properly study the effect of extreme temperatures on plant growth, we have engineered a new device called the Temperature Gradient in the Root Zone (TGRooZ). The TGRooZ generates a controlled temperature gradient in the root growth zone while keeping the aerial tissues exposed to the environmental temperature, generating conditions similar to those in natural ecosystems. This device is adaptable for *in vitro* analyses using agar-based systems on Petri dishes or soil-containing pots for greenhouse experiments. In *in vitro* experiments, we demonstrated that seedlings growing under homogenous high temperatures (applied equally to the shoot and root) develop a significant shorther roots by decreasing cell division in the meristem, induce root stem cell replacement, and block lateral root emergence. Remarkably, although shoots of seedlings growing in the TGRooZ are exposed to a similar high temperature, they recover almost all parameters to values observed in seedlings cultivated at standard temperatures. We also defined the transcriptomic profiles of roots and shoots of plants grown under heat stress (homogeneous 32°C in the shoot and root), at a standard temperature (22°C in the shoot and root), and at 32°C in the TGRooZ. Gene ontology analyses indicated a role for auxin in the heat response of shoots. Genetic analyses showed that auxin is important for the maintenance of shoot growth under high-temperature conditions. We identified genes necessary for normal root growth in response to the gradient of temperature imposed with the TGRooZ. Morphological analyses of the corresponding mutants growing in the TGRooZ showed that root development was not completely recovered, suggesting that the TGRooZ is an important tool for understanding the response to heat in the whole plant. In addition, our results clearly show that a temperature gradient in the root ecosystem has beneficial properties for the plant under heat-stress conditions; it facilitates the recruitment of specific microbial communities and the differential accumulation of mineral nutrients in the plant or modulates specific gene expression, as well as increasing plant biomass production. However, a high homogeneous temperature compromises root growth and functional capacities, reducing plant adaptation to heat stress. Taken together, our data clearly indicate that by cultivating plants with their root system in a temperature gradient in the dark, we can reproduce a growth environment similar to that found in the field. Based on the results presented here, we envision that the use of TGRooZ technology will help researchers to obtain reliable and close-to-field data and improve our understanding of how plants respond to heat stress.

RESULTS

Roots are sensitive to high temperatures

We wanted to analyze the effect of a high temperature over a long period of time on plant growth. First, we noticed that in natural soils, roots normally grow in a lower temperature than aerial plant parts, and this likely protects the root system from excessive high temperatures. In fact, a decreasing temperature gradient is formed from the topsoil to the deeper layers in a natural soil (Supplemental Figure 1A). We analyzed changes in the temperature gradient in the field during day and night periods for 4 days and found that the temperature variations were small (Supplemental Figure 1B and 1C). Taking into account these observations, we engineered a device called the TGRooZ to generate a temperature gradient in the root-growing zone for *in vitro* assays or greenhouse analyses. The TGRooZ consists of a metallic growth box with a cold-regulable bottom container (Supplemental Figure 1D); the temperature difference between the bottom and the top of the device generates a gradient that can be controlled by adjusting the temperature at the bottom (Supplemental Figure 1D–1F). As indicated, the day-night temperature variation at a 5- or 15-cm soil depth was small. Therefore, although the TGRooZ device generates a day-night static gradient, it can offer the advantage of studying the plant response to heat stress in a controlled environment. Seeds of Arabidopsis *SKP2Bp*::*GUS*, a marker line for lateral root primordia formation, were germinated at 22°C, using the D-Root device (Supplemental Figure 1E) to maintain the roots in darkness (Silva-Navas et al., 2015). Four days after germination, seedlings were exposed to either homogeneous 22°C (shoot and root at 22°C: 22SR seedlings), homogeneous high temperature of 32°C (shoot and root at 32°C: 32SR seedlings), or 32°C in the shoot and a temperature gradient in the root zone (32TGRooZ seedlings) (Supplemental Figure 1F)

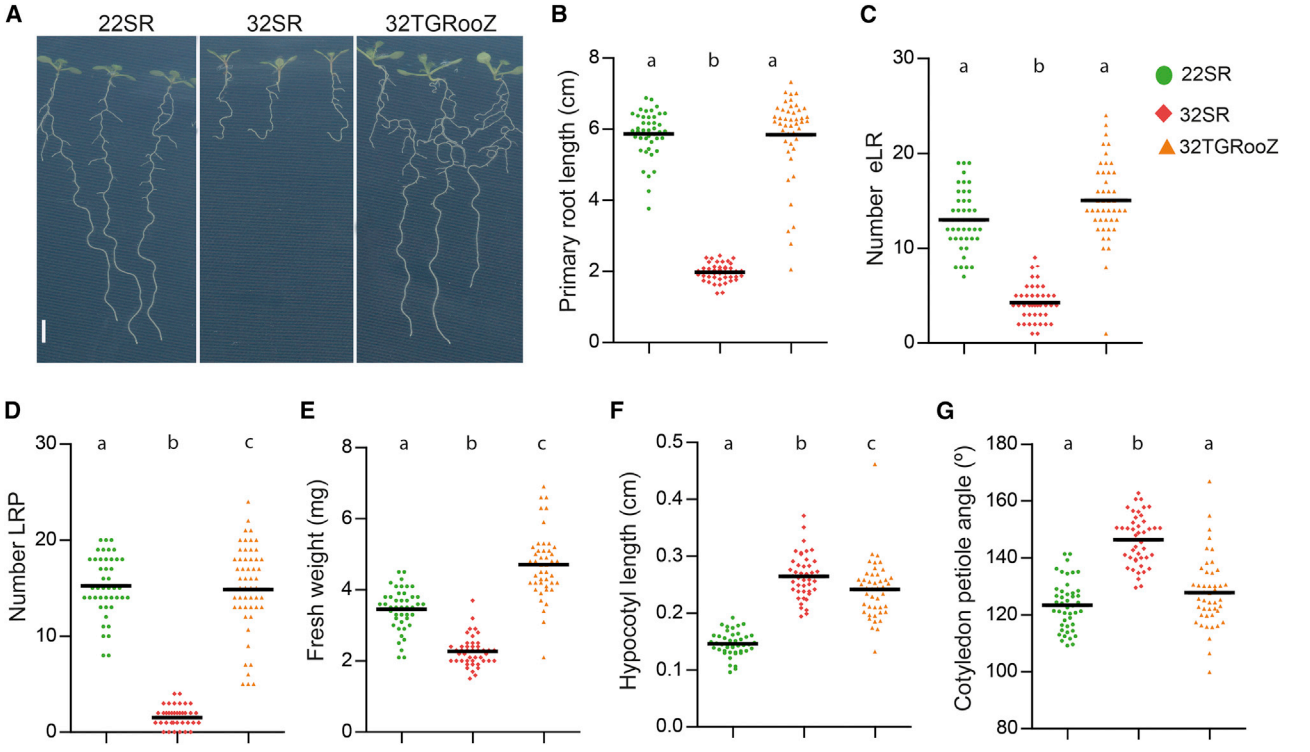

Figure 1. Effect of high temperature and a gradient in the root zone on seedling development.

(A) Representative images of 10-day old Arabidopsis seedlings grown at homogeneous 22°C (22RS), 32°C (32SR), or 32°C in the shoot with the 32TGRooZ. Scale bar, 0.5 cm.

(B) Quantification of primary root length.

(C) Quantification of the number of emerged LRs (eLR).

(D) Quantification of the number of LRP before emergence.

(E) Quantification of the fresh weight per seedling.

(F) Hypocotyl length from the root-shoot junction to the base of the shoot meristem.

(G) Cotyledonary angle. **(B–G)** n ≥ 25. Significance was determined by ANOVA and Tukey's honestly significant difference (HSD) post-test. $p < 0.05$. Different letters indicate significant differences.

for 6 more days. The high-temperature treatment (32SR) significantly decreased root growth (Figure 1A and 1B) and lateral root (LR) number, both the number of emerged LRs (Figure 1C) and that of LR primordia (LRP) (Figure 1D). Consistent with the decrease in LR emergence in 32SR seedlings, we found that, in the root portion growing at 32°C after the transfer, the few LRP that were formed did not progress beyond stage I, whereas LRP developed normally in roots growing at 22°C (22SR) or in a temperature gradient (32TGRooZ) (Supplemental Figure 2). Strikingly, all deleterious root phenotypes associated with heat stress were reversed or improved to different levels in the 32TGRooZ seedlings (Figure 1A–1D).

Shoot responses to prolonged heat stress depend partially on root growth

We also analyzed the effect of prolonged high temperatures on shoot development using the TGRooZ. We found that 32SR plants produced a lower shoot biomass (Figure 1E). However, the shoot biomass of 32TGRooZ seedlings was higher than that of 22SR (Figure 1E), indicating a positive effect of high temperatures on shoot growth when the root system was growing in the TGRooZ device. We also quantified the elongation of the hypocotyl and the cotyledonary petiole angle, two responses associated with increased temperature in Arabidopsis (Gray et al., 1998; Sun et al., 2012). The hypocotyl length of 32SR seedlings increased by more than 80% compared with 22SR, whereas the increase in 32TGRooZ seedlings was slightly smaller (Figure 1F). The cotyledonary petiole angle was significantly bigger in 32SR seedlings than in 22SR or 32TGRooZ seedlings (Figure 1G). These results demonstrate that the impairment of root development linked to high temperatures modulates some responses in the shoot, such as biomass production or the cotyledonary petiole angle, but not hypocotyl elongation, a response that seems to be independent of root temperature.

We also analyzed the effect of heat and soil-root temperature on plants growing in pots that contained soil. To do this, the TGRooZ was adapted to hold soil-containing pots (Supplemental Figure 1G) and generate a temperature gradient along the soil layers (Supplemental Figure 1H). First, we tested the effect of high temperature on leaf transpiration and leaf temperature. We observed that 32SR plants had reduced stomatal conductance compared with 22SR control plants, and the conductance levels were restored in 32TGRooZ plants even though their leaves were also growing at 32°C (Supplemental Figure 3A). For these experiments, the soil water

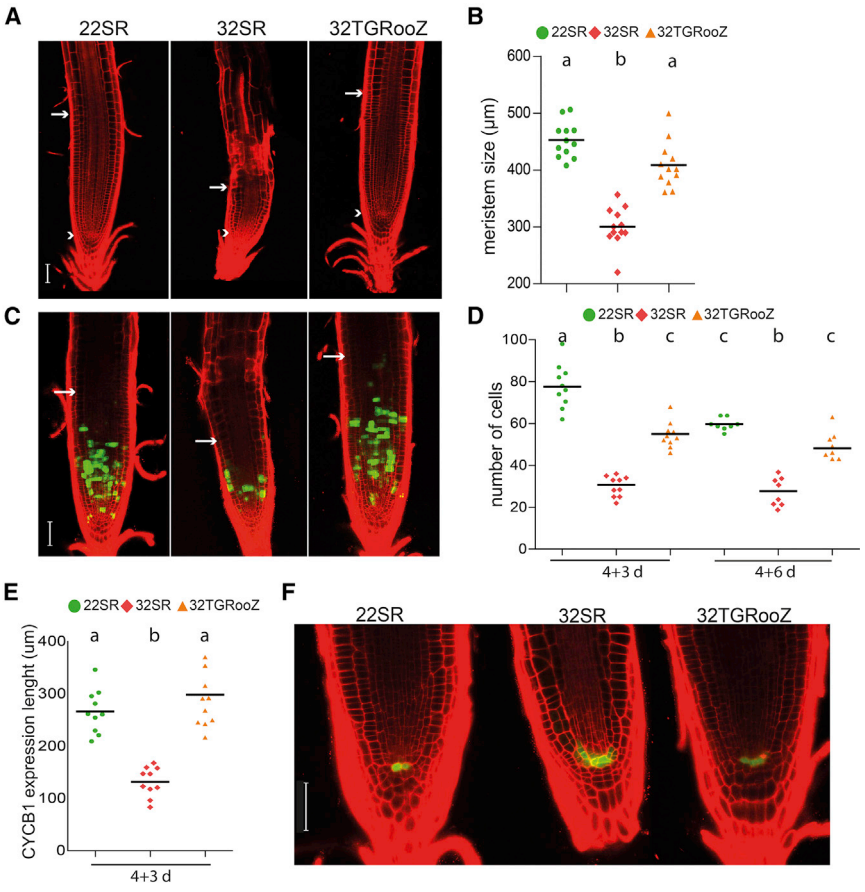

Figure 2. High temperatures decrease cell division but activate QC proliferation.

(A) Confocal images of root meristems of 22RS, 32SR, or 32TGRooZ seedlings grown for 6 days after the transfer. White arrowheads indicate the QC, and arrows indicate the end of the meristem. Scale bar, 50 μm.

(B) Meristem size from the QC to the last dividing cell (n = 12).

(C) Confocal images of a z-stack of PI-stained RAMs from 22SR, 32SR, or 32TGRooZ *CYCB1;1:CYCB1;1-GFP* seedlings grown for 6 days after transplant. White arrows indicate the end of the meristem. Scale bar, 50 μm.

(D) Number of cells showing a GFP signal at 3 days (n = 10) or 6 days (n = 8) after transfer to different temperatures.

(E) CYCB1;1 expression domain in the root apical zone of seedlings grown for 6 days after transfer at different temperatures.

(F) Confocal images of the QC labelled with the WOX5p:GFP marker 6 days after transfer to 22SR, 32SR, or 32TGRooZ conditions. Scale bars, 50 μm. Significance was analyzed by ANOVA and Tukey's honestly significant difference (HSD) post-test. $p < 0.05$. Different letters indicate significant differences.

content was maintained at similar levels across all treatments (Supplemental Figure 4), ensuring that the decrease in stomatal conductance was not due to water scarcity in the soil. We also found that the leaves of 32SR plants had a significantly higher temperature than those of 22SR or 32TGRooZ plants (Supplemental Figure 3B and 3C). Although the recovery was not total, leaves from 32TGRooZ plants were more efficient in downregulating their temperature than those from 32SR (Supplemental Figure 3B and 3D). These data indicate that leaf temperature is influenced by both atmospheric and root-zone temperatures.

To generalize the temperature-dependent root growth phenotypes to other plant species, we carried out similar analyses in tomato plants using a modified TGRooZ device and increasing the temperature from 26°C (optimal for tomato in *in vitro* assays) to 34°C (Supplemental Figure 5A). We found that root growth and the number of LRs were significantly decreased when plants were exposed to homogeneous high temperatures of 34°C (34SR) compared with 26°C (26SR), as occurred in Arabidopsis (Supplemental Figure 5B). Likewise, when tomato plants were cultivated at 34TGRooZ, root growth and LR number were slightly increased. Compared with 26SR tomato seedlings, shoot and root biomass were decreased in 34SR seedlings, but the biomass was unchanged in 34TGRooZ (Supplemental Figure 5B). These data indicate that tomato root and shoot growth are also sensitive to excessively high temperatures, and the use of TGRooZ can generate a better environmental condition to study heat stress in crops.

High temperature affects cell division in the root apical meristem

Next, we decided to investigate the causes of the root growth reduction in response to heat by analyzing the structure of the Arabidopsis root apical meristem (RAM). The RAM of 32SR seedlings showed a significantly smaller meristem size with fewer dividing cells that expressed the cell division marker *CYCB1;1:CYCB1;1-GFP* (Ubeda-Tomas et al., 2009) compared with 22SR plants (Figure 2A and 2B). The Arabidopsis root meristem size was larger in 32TGRooZ than 32SR seedlings, but it did not completely recover the size of 22SR. These results indicate that a temperature gradient promotes optimal root growth, but some other signals may also control the size of the meristem.

Delving deeper, we explored whether the decrease in root meristem size observed at high temperature could derive from defects in the stem cell niche. The quiescent center (QC), located in the RAM, harbors a group of cells with a low division rate that replenish the stem cell niche (Dolan et al., 1993; Cruz-Ramírez et al., 2013). Interestingly, using the WOX5:GFP marker to visualize QC cells, we found more WOX5:GFP-expressing cells in 32SR seedlings compared with 22SR or 32TGRooZ seedlings (Figure 2C), indicating that QC cell division was activated in response to heat stress, likely to replace meristematic stem cells that prematurely stopped proliferation or were damaged because of the stress.

A temperature gradient in the root growth zone is required to maintain optimal levels of *ERF115* in the RAM

ERF115 is a transcription factor that promotes cell renewal after stem cell damage and responds to moderate changes in root

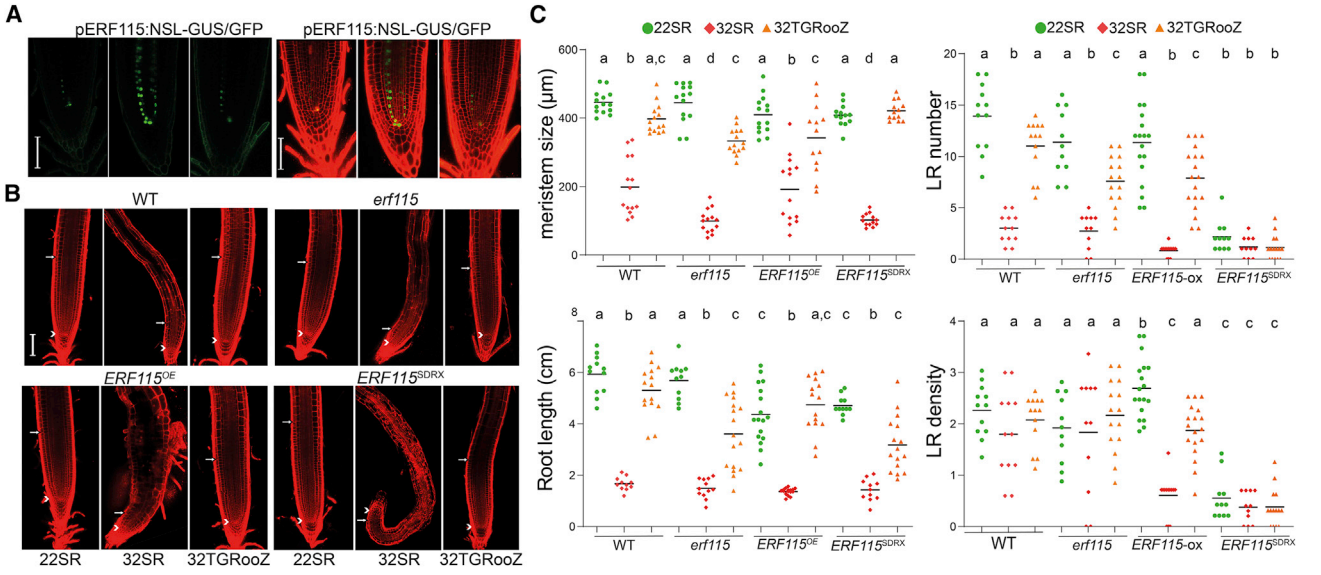

Figure 3. *ERF115* is needed for root growth recovery in the TGRooZ.

(A) Confocal images of meristems of 22SR, 32SR, and 32TGRooZ pERF115:NSL-GUS/GFP. (Left) GFP-tagged expression in green. (Right) GFP overlapped with PI-stained roots. Scale bar, 50 μm.

(B) Confocal images of PI-stained root meristems of 22SR, 32SR, and 32TGRooZ wild type (WT), *erf115* mutant, *ERF115* over-expressing (*ERF115*^{OE}), or ERF115^{SDRX} seedlings. White arrowheads indicate the QC, and arrows indicate the end of the meristem. Scale bar, 100 μm.

(C) Quantification of root meristem size (n > 12), root length, number of LRs, and lateral root density of 22SR, 32SR, or 32TGRooZ WT, *erf115* mutant, *ERF115*^{OE}, or ERF115^{SDRX} seedlings at 6 days after transfer to different temperatures (n ≥ 12). Significance was analyzed by ANOVA and Tukey's honestly significant difference (HSD) post-test. $p < 0.05$. Different letters indicate significant differences.

temperature to control cell division and stem cell replenishment in the QC (Heyman et al., 2013). Using the D-Root system to grow roots in darkness, we found that *pERF115:NLS-GUS/GFP* was slightly expressed in QC cells and vascular cells of 22SR seedlings (Figure 3A). However, this expression significantly increased in response to 32°C in QC, vasculature, and pericycle cells. By contrast, the expression of *ERF115* in 32TGRooZ seedlings was similar to that in 22SR (Figure 3A), indicating a local response to the temperature in the root growth zone. The loss-of-function *erf115* mutant grown at 22°C showed root meristem size and root length similar to those of 22SR wild-type (WT) seedlings. However, at 32°C, the root meristem size of *erf115* was significantly smaller (Figure 3B and 3C). Furthermore, the meristem size recovery of 32TGRooZ was limited for *erf115* (72%) compared with WT seedlings (90%) (Figure 3C). This effect might be due to a higher sensitivity of the *erf115* root meristem to the temperature variations generated along the gradient, correlating with a reduction in root growth of the mutant. As expected, WT and *erf115* seedlings showed a similar trend in the number of emerged LRs in response to changes in temperature in the root zone (Figure 3C), as mutation of *ERF115* does not seem to affect the number of emerged LRs (Canher et al., 2021). However, over-expression of *ERF115* slightly increases the LR density, a parameter that is not fully recovered in the TGRooZ. Whether this decrease is due to a decrease in LR emergence or LR specification is not known and should be analyzed in the future. It is possible that, in response to high temperatures, over-expression of *ERF115* activates a response that decreases cell division in the primordia and slows LR emergence.

Root temperature drives transcriptional response to heat stress in the plant

Based on our observations, we hypothesized that plant molecular responses to high temperature might be influenced by the temperature in the root zone. To demonstrate this, we carried out comparative pairwise transcriptomic analysis of shoots or roots from WT Arabidopsis seedlings grown under 22SR, 32SR, and 32TGRooZ conditions. We found that high temperatures of 32°C compared with 22°C had a strong effect on gene expression in both root and shoot, affecting more than 7000 genes (Supplemental Table 1A–1F), including many transcription factors (Supplemental Table 1G). Interestingly, 34 of them belong to the ERF family, indicating that this family probably plays an important role in the response to heat, as demonstrated above by the function of *ERF115*. Hierarchical clustering of the genes with the greatest variance showed that gene expression in the roots of 32SR seedlings was significantly different from that in roots of 22SR or 32TGRooZ seedlings (Supplemental Figure 6A and Supplemental Table 1A–1C). Gene ontology analyses of differentially expressed genes in the root showed an enrichment in heat stress, water deficiency, response to temperature, RNA modification, oxidative stress, and response to hypoxia, among many other terms (Figure 4A). We also noticed that gene expression in the shoot of 32SR or 32TGRooZ seedlings was significantly different from that in the shoot of 22SR seedlings (Supplemental Figure 6B and Supplemental Table 1D–1F). Gene ontology analyses of differentially expressed genes in the shoot showed an enrichment in photosynthesis, light and auxin signaling, response to temperature, and protein folding, among other categories (Figure 4B). Interestingly, although the shoots of 32SR and 32TGRooZ seedlings were grown at similar high

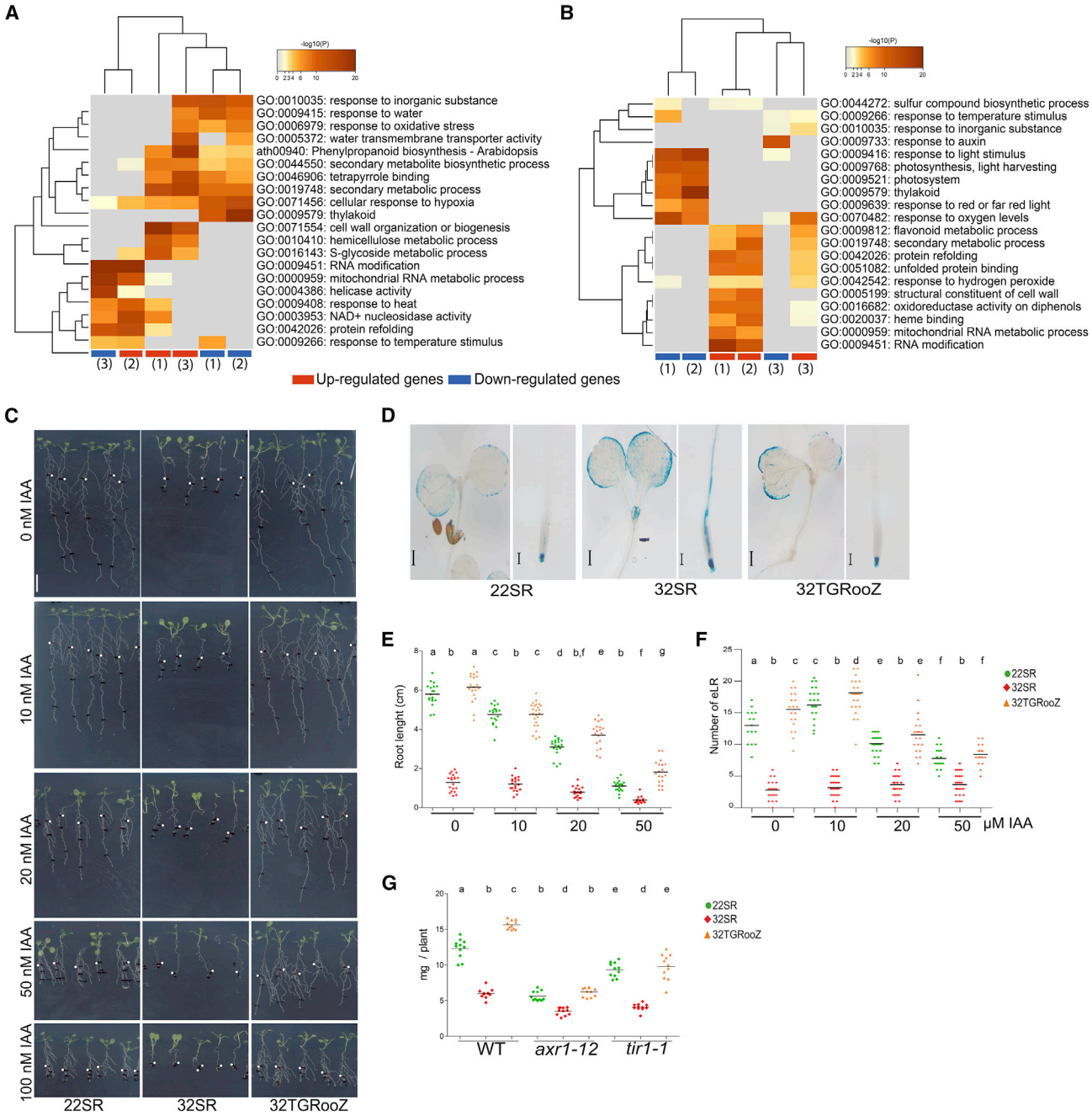

Figure 4. Temperature gradient in the root zone modifies gene expression in roots and shoots in response to heat.

Gene ontology category heatmap of genes differentially expressed in roots **(A)** or shoots **(B)** in response to temperature. (1) 32TGRooZ vs 22SR; (2) 32SR vs. SR22; and (3) 32SR vs. 32TGRooZ comparisons. Red and blue boxes correspond to induced and repressed genes, respectively.

(C) Representative pictures of DR5:GUS seedlings grown for 4 days at 22°C and then transferred to fresh medium containing 0, 10, 20, 50, or 100 nM indole acetic acid (IAA, auxin) and to 22°, 32°C, or 32TGRooZ for 6 more days. The white dots indicate the point of the RAM at the transfer. Scale bar, 1 cm.

(D) Shoot and root apical zone of DR5:GUS seedlings grown as in (**C**) and stained for GUS activity. Scale bar, 400 μm for shoot pictures and 100 μm for root pictures.

(E) Root length of seedlings grown as in (**C**).

(F) Number of LRs of seedlings grown as in (**C**).

(G) Fresh weight of WT, *axr1-12*, or *tir1-1* grown for 4 days at 22°C and then transferred to 22SR, 32SR, or 32TGRooZ conditions for 6 additional days. Significance was analyzed by ANOVA and Tukey's honestly significant difference (HSD) post-test. $p < 0.05$. Different letters indicate significant differences.

temperatures, almost 700 genes showed a significantly different expression level (Supplemental Table 1F). These genes were enriched in auxin response, oxygen levels, protein refolding, and response to nutrient starvation and iron transport, among other terms (Supplemental Figure 6C and Supplemental Table 1F). Because auxin regulates growth, we decided to analyze the role

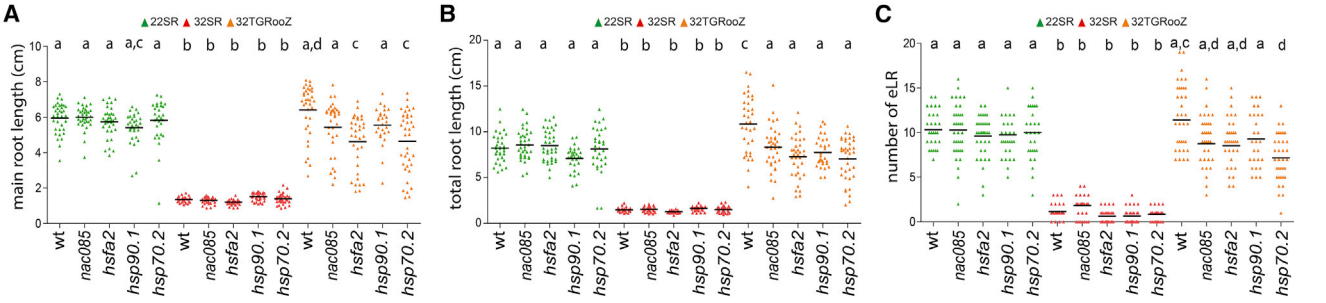

Figure 5. Effect of high temperature and a temperature gradient in the root zone on heat-response mutants.
(A) Root lengths of 22SR, 32SR, and 32TGRooZ WT and mutant seedlings.
(B) Total root length (main plus LR length) of 22SR, 32SR, and 32TGRooZ WT and mutant seedlings.
(C) Number of emerged LRs of 22SR, 32SR, and 32TGRooZ WT and mutant seedlings ($n \geq 24$). Significance was analyzed by ANOVA and Tukey's honestly significant difference (HSD) post-test. $p < 0.05$. Different letters indicate significant differences.

of this hormone in response to high temperature. First, using the DR5:GUS marker, we found higher GUS activity in both shoot and root apical areas of seedlings grown at homogeneous 32°C compared with 22SR seedlings (Figure 4D). Interestingly, this higher GUS activity was decreased in 32TGRooZ seedlings to basal levels, even when the shoots were exposed to high temperatures. These data indicate that auxin signaling in response to heat stress, in both shoots and roots, is influence by the temperature in the root zone. This DR5:GUS activation correlates with the lower expression of some Aux/IAA and SAUR genes in the shoots of the 32SR seedlings (Supplemental Table 1F), which could negatively regulate the auxin response (Powers and Strader, 2020) and growth, respectively (Ren and Gray, 2015; Stortenbeker and Bemer, 2018). In addition, we found that a combination of exogenous auxin application and high temperature enhanced the root growth inhibition phenotype. However, this root growth inhibition was lower in 32TGRooZ seedlings supplemented with 20 or 50 nM of auxin than in roots from 22SR or 32SR seedlings (Figure 4E). Furthermore, we found that a low concentration of exogenous auxin (10 nM) increased LR emergence in 22SR or 32TGRooZ seedlings but not in 32SR seedlings (Figure 4F). We also analyzed the effect of high temperature on *axr1-12* (Lincoln et al., 1990) and *tir1-1* (Ruegger et al., 1998), two mutants with decreased auxin signaling. In contrast to WT plants, neither mutant showed an increase in shoot growth when cultivated at 32TGRooZ compared with 22SR (Figure 4G). Taken together, our data suggest that correct auxin signaling is needed for shoot growth in response to heat and that shoot responses to high temperatures are partially influenced by soil-root temperature and seem to be mediated, at least in part, by auxin signaling.

Chaperone function modulates root development under heat stress

In the transcriptomic comparisons, we identified genes involved in the response to extreme temperature that were induced in both roots and shoots in all comparisons (32SR vs 22SR, 32SR vs 32TGRooZ, and 32TGRooZ vs 22SR) (Supplemental Figure 7A and 7B, Supplemental Table 1J). A gene ontology analysis of this gene set identified protein folding as a common functional category (Supplemental Figure 7C and 7D). Among the induced root and shoot common genes, we identified the *HSFA2* transcription factor and the two heat shock proteins (HSPs) *HSP90.1* and *HSP70.2*, which are involved in stress responses, thermomemory, and protein folding (Schramm et al., 2006; Wang et al., 2016; Leng et al., 2017; Friedrich et al., 2021), as well as the *NAC085* transcription factor, which is involved in G2 arrest in response to heat stress (Takahashi et al., 2019). Interestingly, a gene network identified several *HSP* genes as targets of *ERF115*, including HSP90.1 (Supplemental Figure 7E), suggesting a direct connection between *ERF115* and the heat responses mediated by HSPs. Analyses of the homozygous mutants for these genes at 22°C showed that their primary root length was similar to that of WT seedlings (Figure 5A). At 32°C, root growth was severely compromised in all genotypes (Figure 5A). Using the TGRooZ, we found that the root growth of *nac085* and *hsp90.1* seedlings recovered to levels similar to WT plants, while the root length of *hsf2a* and *hsp70.2* remained significantly smaller (Figure 5A), indicating that they may function in the control of main root growth during heat stress. A similar trend was observed for total root length (length of primary root and LRs), but for this trait, the recovery was significantly smaller in all mutants compared with WT plants (Figure 5B), indicating an important role of chaperones in LR growth. Indeed, the LR number was significantly decreased by the effect of high temperature in all genotypes (Figure 5C), but this parameter was not fully recovered in these mutants when grown at 32TGRooZ, except for *hsp90.1* (Figure 5C). By contrast, when growing in 32TGRooZ, the *hsp70.2* mutant showed a significantly lower number of LRs than control seedlings (Figure 5C), suggesting an important role of this gene in LR development under heat stress.

We also analyzed the effect of the different temperature treatments on hypocotyl length (Supplemental Figure 8A) and cotyledonary petiole angle (Supplemental Figure 8B) in these mutants. In general, we did not find any significant difference in either response between WT plants and mutants in the 22SR, 32SR, or 32TGRooZ treatments, with the exception of the *hsfa2* mutant, which did not increase the cotyledonary petiole angle in response to heat (32SR) (Supplemental Figure 8B). These data suggest that *HSFA2* functions in the leaf hyponastic response needed to elevate the cotyledons from the soil in response to heat.

Heat stress affects plant phosphate nutrition

To better understand the influence of the TGRooZ on the plant transcriptome, we overlapped the differentially expressed genes

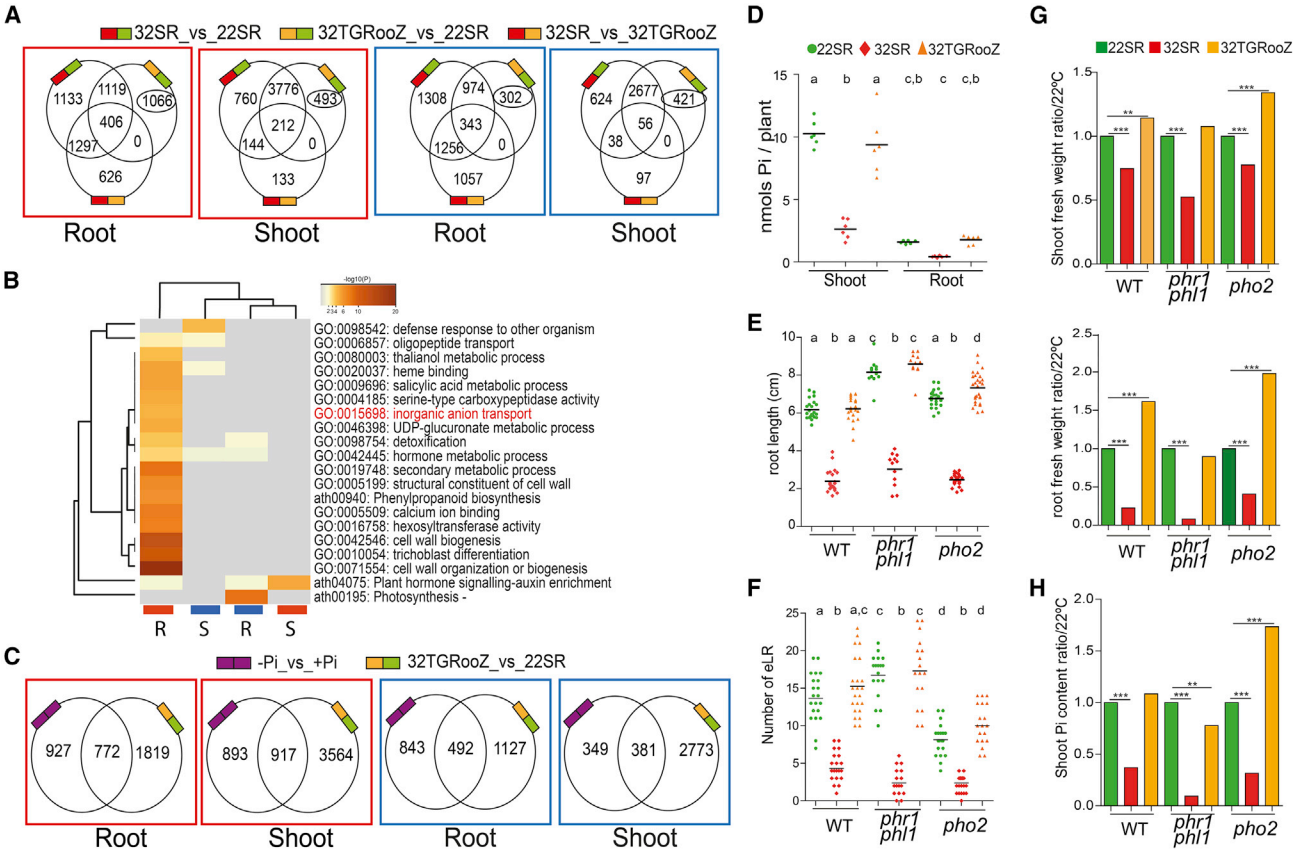

Figure 6. High temperatures affect Pi nutrition.

(A) Venn diagrams of differentially expressed genes (DEGs) between different comparisons (up- or downregulated genes) in roots or shoots. Circled numbers indicate the number of genes specifically deregulated between 32TGRooz and 22SR but not under other conditions.

(B) Gene ontology (GO) heatmap of specific genes (circled in A) in roots (R) or shoots (S) that were up- or downregulated (red and blue rectangles, respectively).

(C) Venn diagrams of DEGs deregulated by Pi starvation and by the effect of temperature between 32TGRooZ and 22SR in both roots and shoots. Red and blue boxes correspond to up- and downregulated genes, respectively.

(D) Free Pi level in roots or shoot of SR22, SR32, or 32TGRooZ Arabidopsis seedlings grown in a medium containing Pi for4 days and then transferred to different temperatures for 6 additional days. Values correspond to nmoles Pi per plant.

(E and F) Root length **(E)** and emerged LRs (eLR) **(F)** in WT, *phr1 phl1*, or *pho2* mutants grown for 4 days at 22°C and then transferred to 22SR, 32SR, or 32TGRooZ conditions for 6 additional days. Significance was analyzed by ANOVA and Tukey's honestly significant difference (HSD) post-test. Different letters indicate significant differences.

(G) Shoot or root fresh weight of WT, *phr1 phl1*, or *pho2* mutants grown for 4 days at 22°C and then transferred to 22SR, 32SR, or 32TGRooZ conditions for 6 additional days. Values are expressed relative to those at 22°C.

(H) Shoot Pi level (nmoles/plant) in WT, *phr1 phl1*, or *pho2* mutants grown as in (**G**). Values are expressed relative to those at 22°C. Asterisks indicate significant differences with respect to 22°C by t-test. **p < 0.01; ***p < 0.001.

between all comparisons among treatments (Figure 6A and Supplemental Table 1H). We focused on those genes that were differentially expressed in root and shoot between 22SR and 32TGRooZ experimental conditions because they were most likely to reflect the response to a heat wave in a natural field. Gene ontology analyses showed an enrichment in terms related to hormone signaling (auxin and salicylic acid), the cell wall, and anion transport, among others (Figure 6B). Analyzing the inorganic anion transport category, we found several phosphate (Pi) transporters, an observation that is in agreement with the suggested interconnection between Pi and temperature (Pacak et al., 2016; Giri et al., 2017; Singh et al., 2018). Furthermore, we found a significant overlap between genes deregulated by Pi starvation in roots (Silva-Navas et al., 2019) and shoots (del Pozo, unpublished) and genes deregulated by heat stress in both roots and shoots (Figure 6C and Supplemental Table 1I). Among them, we found several Pi starvation transporters and signaling genes that were upregulated by the effect of heat (Supplemental Figure 9A and Supplementary Table 1I). A recent study reported a curated collection of genes (the known ionome gene [KIG] list) that were experimentally demonstrated to participate in uptake, accumulation, or distribution of mineral nutrients in plants (Whitt et al., 2020). We found a significant overlap between this KIG gene set and our temperature-deregulated gene set (Supplemental Table 2). Remarkably, *PHR1* and *PHL1*, two key regulators of the Pi response, and *PHO2*, a regulator of Pi transport to the xylem, were downregulated in response to heat in almost all comparisons (Supplemental Figure 9A), whereas several Pi transporters were upregulated in roots or shoots in

response to heat (Supplemental Figure 9B). It is likely that the plant differentially adjusted the expression of these Pi starvation response regulators and transporters to establish a new Pi homeostasis during heat stress. Next, we measured the cellular free Pi content in plants exposed to the different temperature treatments. We found that Pi levels in 32SR seedlings were significantly lower, in both shoots and roots, than those in 22SR seedlings (Figure 6D). Interestingly, Pi levels were recovered in both shoots and roots of 32TGRooZ seedlings (Figure 6D), indicating that, during heat stress, correct Pi homeostasis is maintained if the roots are cultivated in a dark environment with a temperature gradient. We analyzed the effect of heat stress on the *phr1 phl1* double mutant, which exhibits a decreased Pi starvation response (Bustos et al., 2010), and *pho2*, which shows an over-loading of Pi from root to shoot (Liu et al., 2012). We found that the heat response of the *phr1 phl1* mutant was similar to that of WT plants in terms of root length and LR emergence (Figure 6E, 6F and Supplemental Figure 9C). However, *pho2* root elongation (but not LR number) was recovered in the TGRooZ and was higher than that of WT seedlings (Figure 6E and 6F). The shoot weight of the *phr1 phl1* mutant showed less recovery in TGRooZ than that of control seedlings, whereas the shoot weight of the *pho2 mutant* showed significantly higher recovery, consistent with its higher shoot Pi content (Figure 6G). This phenotype was more noticeable in the recovery of root biomass (Figure 6G). Interestingly, the amount of free Pi was significantly decreased in the *phr1 phl1* mutant in response to heat, probably because it was unable to fully activate the Pi starvation response, whereas Pi accumulation in the *pho2* mutant increased when it was grown in the TGRooZ. Taken together, these data suggest that a reduction in Pi responses or lower Pi accumulation contributes, at least in part, to the decrease in shoot growth during heat stress.

High temperature in the root system affects bacterial community assembly and root functionality

To further understand the relationship between high temperature and root function, we compared the bacterial community composition and ionome of tomato plants whose root growth was limited by excessive high temperature. Tomato seedlings were grown in natural soil and exposed to three different temperature regimes: 22SR, 36SR, and 36TGRooZ (a root temperature gradient that partially mimicked real soil conditions). We determined their shoot mineral nutrient accumulation (ionome) and found that, in general, mineral nutrient accumulation patterns were similar in 22SR and 36TGRooZ leaves but differed in SR36 leaves (Supplemental Figure 10A). Consistent with the transcriptional analysis, in which the expression of several ion transporters was deregulated, different temperature regimes altered the levels of various mineral nutrients in leaves, including P, Cu, B, Mo, As, Rb, and K (Supplemental Figure 10B). These results suggest that changes in tomato mineral nutrition are influenced by soil temperature and likely by root functionality.

We compared bacterial community profiles in the rhizosphere and root using 16S rRNA amplicon sequencing. Across all temperatures used, soil and rhizosphere samples supported higher bacterial alpha diversity and richness indexes compared with roots (Supplemental Figure 11A and 11B), a difference that has been systematically observed in natural environments where the species richness is lower in the plant than in the soil (Castrillo et al., 2017; Finkel et al., 2019).

As in previous experiments (Castrillo et al., 2017; Finkel et al., 2019), the original soil (inoculum), rhizosphere, and roots assembled diverse bacterial communities; the differences among these fractions explained most of the variance in community composition (Supplemental Figure 12A). Compared with the rhizosphere and soil fractions, the tomato root samples were mainly enriched in Proteobacteria and Bacteroidetes and depleted in Acidobacteria, Gemmatimonadetes, Firmicutes, Chloroflexi, and Verrucomicrobia (Supplemental Figure 12B and 12C). Consistent with the ionomic data, we noticed that the bacterial profile in roots of high-temperature-treated plants (36SR) differed from that of 22SR and 36TGRooZ plants (Supplemental Figure 12B and 12C). Furthermore, 36SR tomato roots showed a clear increase in Actinobacteria, a phylum that is normally decreased in healthy roots (Castrillo et al., 2017; Finkel et al., 2019) (Supplemental Figure 12B and 12C).

We further investigated the effect of high temperature on root bacterial community composition. Canonical analysis of principal coordinates showed significant differences in root bacterial community composition across the temperature treatments (Figure 7A). These differences were robust in both fractions, the rhizosphere and the root (Figure 7A and 7B). We noticed that the rhizosphere and root microbiome compositions were similar in tomato 22SR and 36TGRooZ plants and differed significantly from those of 36SR plants (Figure 7). This observation was consistent at different phylogenetic levels (Figure 7C and 7D), indicating that high temperature in the soil, but not in the shoot (comparison between 36SR and 36TGRooZ), influences the capacity of the root to assemble an intact microbiome. The high-temperature effect of 36°C on root microbiome composition and plant mineral nutrient accumulation, in contrast to 22°C or TGRooZ in heat-stressed plants, emphasizes the protective role of the soil in buffering high temperature fluctuations to preserve root function. Taken together, these results suggest that changes in the root function of tomato are likely to be a direct consequence of high temperature on the soil, the alterations in the microbiota, or the interaction of both.

DISCUSSION

In this work, we used a novel approach that reflects natural soil properties in many aspects to demonstrate that a temperature gradient in the root ecosystem is essential for studying and understanding the whole-plant response to heat stress. In general, *in vitro* and greenhouse studies have not considered the temperature in the root zone when analyzing the effect of heat stress (Heckathorn et al., 2013; Valdés-López et al., 2016; Chen and Li, 2017; Estravis-Barcala et al., 2021; Pei et al., 2021). In response to warming temperatures, which are normally optimal and non-detrimental for plant growth, one of the thermomorphogenetic responses is the elongation of roots. By contrast, when entire plants are cultivated at high temperatures (above optimal), root growth is arrested and LR formation is blocked, decreasing root functionality and negatively affecting shoot biomass. Here, we present robust data showing that a high temperature in the root growing zonehas a strong impact on plant development, physiological

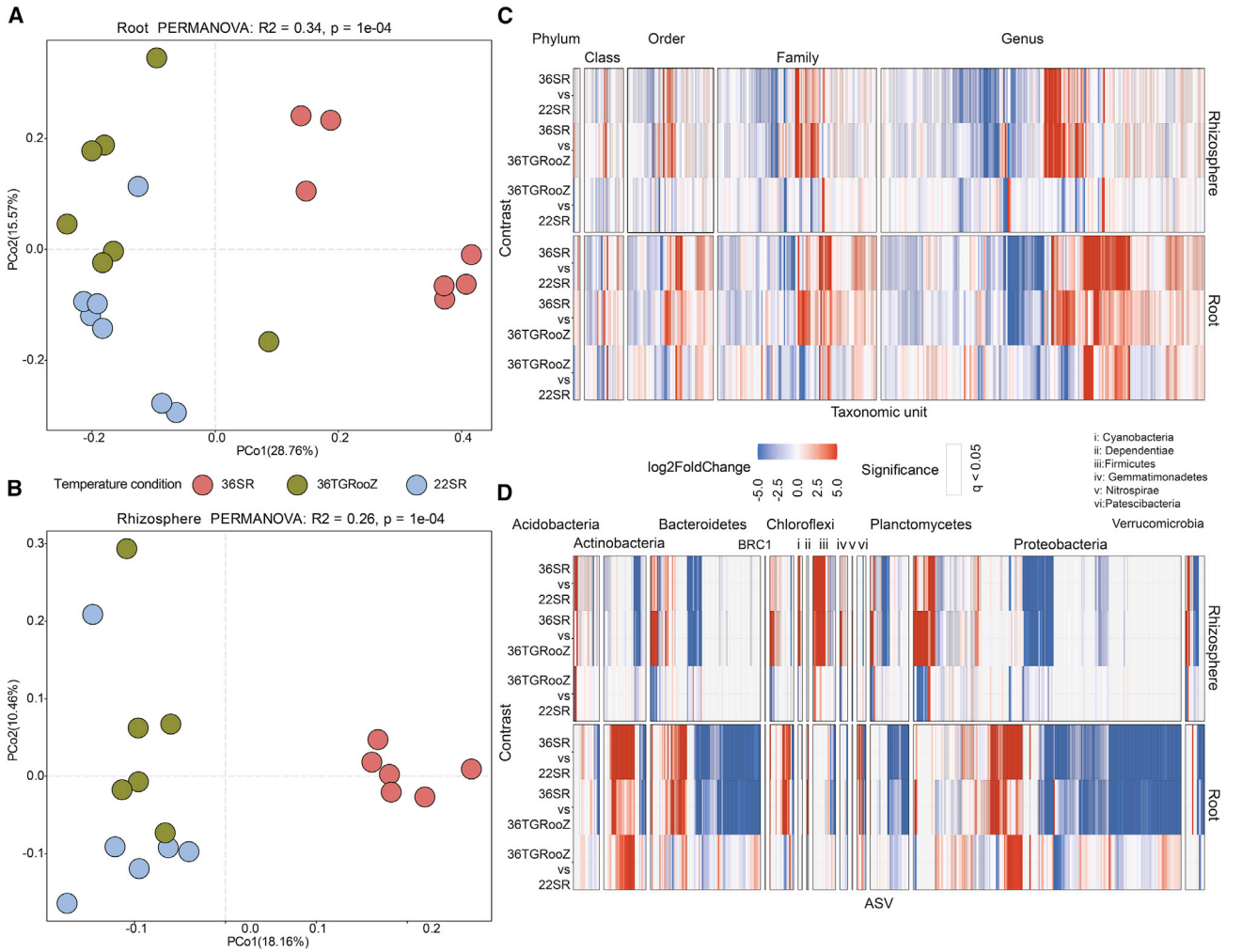

Figure 7. High soil temperatures select different rhizosphere and root microbiome compositions.

Rhizosphere and root microbiome compositions of tomato plants grown at 22°C (22SR) and 36TGRooZ are similar, and both are significantly different from the microbiomes found in plants grown at 36°C (36SR).

(A) Principal coordinate analysis (PCoA) based on Bray-Curtis dissimilarities between bacterial communities in roots or **(B)** rhizospheres of tomato plants grown at 22°C (22SR), 36°C (36SR), or 36TGRooZ for 4 weeks.

(C) Heatmaps showing root and rhizosphere enrichment patterns of different taxonomic units (phylum, class, order, family, genus) or (**D**) amplicon sequence variants (ASVs) across all versus all contrasts between temperature conditions used in (**A**). The cells of the heatmaps are colored based on the log2 fold change estimated from a generalized linear model contrasting the abundance of each taxonomic unit at each temperature with respect to another in each contrast. Squares outlined in black represent taxonomic units at each taxonomic level that were significantly enriched (red) and depleted (blue) in each comparison ($q < 0.05$).

and molecular responses, and microbiome assembly. The TGRooZ provides a novel and useful approach for studying heat stress in the shoot and roots. This approach can help to identify new solutions and facilitate plant breeding programs to obtain more heat-tolerant crops or to test new microbes to enhance plant tolerance to heat under closer-to-field conditions. Thus, the knowledge generated using the TGRooZ can be useful for coping with the negative effects of global warming and heat waves on crops.

Soil temperature in the root growing zone is important for plant growth and development

In natural ecosystems, soil temperature is affected by several factors, such as environmental temperature, water content, soil compaction, and organic material, among others (Elias et al., 2004). Soil temperature affects many soil physical-chemical properties and living processes that have an impact on plant growth and environmental adaptation (onwuka, 2018; Smith, 2000). A recent work found that soil surface temperature increases, proportionally, more rapidly than air temperature (Zhang et al., 2016). This work predicted that soil respiration will increase by up to 28%, reinforcing the idea that climate warming affects the soil ecosystem and perturbs plant growth. To analyze the effect of heat on soil temperature, in July 2019 in Spain (with an average atmospheric temperature of 34°C but with heat wave peaks over 40°C), we measured the temperature of natural soil at different depths from the top surface down to 14 cm in order to estimate the temperature gradient that formed naturally in the soil. However, we

should take into account that this gradient will depend on physical soil characteristics such as humidity or compaction, among others. We observed that a decreasing temperature gradient was formed in the root growth zone (Supplemental Figure 1A). These data were used to engineer the TGRooZ device that generates a temperature gradient in the plant growth substrate (agar-containing plates or soil) to simulate natural conditions during a heat wave in an enclosed ecosystem (plant growth chamber or greenhouse), where we can control the environmental temperature. In addition, we measured the day-night fluctuation over 4 days in a natural soil in Spain in June 2022. We found that the soil has a stronger temperature buffering capacity at a 15-cm depth than at a 5-cm depth, whereas the temperature fluctuation is significantly greater at the top surface (Supplemental Figure 1B and 1C). This is in agreement with soil thermal diffusivity analyses showing that superficial soil (5 cm) experiences greater temperature variation, whereas at 15 cm or below, temperature changes are buffered across the different seasons (Brunetti et al., 2021). Using the TGRooZ, we provide strong evidence that the soil-root temperature is essential for the plant to activate a full response to heat, conditions that cause severe cellular damage and organ failure (Hasanuzzaman et al., 2013; Qi and Zhang, 2020; Liu et al., 2022). However, the severity of the damage depends on the species, the genotype, and the context of the stress, as these responses are different if the plant encounters gradual temperature variation or if it suddenly faces a high-temperature wave (Larkindale and Vierling, 2008; Gomaa et al., 2011; Zhang et al., 2015). During their lifetime, roots face many hostile environmental conditions that affect growth and development. In response to high temperatures, plants decrease root growth and root meristem size *in vitro* (Yang et al., 2017; Liu et al., 2022). It was reported that heat stress shortens the cell elongation zone, decreasing cell flux from the meristem to the elongation area and stopping root growth (Baskin et al., 1992), likely by decreasing cell division in the root meristem. We found similar phenotypes in plants exposed to a shoot-root homogeneous temperature of 32°C. However, if seedlings were grown in a TGRooZ, with conditions more similar to the field, root growth was not affected, and meristem size was recovered to the level found at optimal temperatures. Hypocotyl elongation, a trait associated with warming (Gray et al., 1998; Bellstaedt et al., 2019; Gaillochet et al., 2020; Lee et al., 2021b), was the unique parameter that was slightly recovered in TGRooZ plants. This suggests that this response mainly depends on the atmospheric temperature surrounding the shoot, although the root temperature can partially influence it.

The gene expression response to heat is strongly conditioned by root temperature (Figure 4). Here, we show that the gene expression of shoots exposed to high temperature is modified when the root system is cultivated in a temperature gradient. It should be noted that many of these differentially expressed genes are related to auxin signaling and are downregulated in plants subjected to homogeneous 32°C compared with those growing in the TGRooZ. A large portion of these genes correspond to members of the SAUR family that are involved in growth control mediated by auxin (Stortenbeker and Bemer, 2018). Auxin plays an essential role in shoot growth and biomass production (Tivendale and Millar, 2022) and heat stress-induced thermomorphogenetic responses, including hypocotyl elongation and leaf hyponasty (Gray et al., 1998; Küpers et al., 2020). Thus, a decrease in auxin signaling might explain, at least in part, the observed decrease in shoot biomass. In this sense, *axr1-12* and *tir1-1*, two mutants with impaired auxin responses, do not fully recover the shoot growth, suggesting an important role of auxin in this process during heat stress. It should be noted that auxin responses require the activity of HSP90 because this chaperone stabilizes TIR1, one of the auxin co-receptors, at high temperatures (Wang et al., 2016), thereby connecting heat stress and auxin signaling. We found that several chaperones, including HSP90.1, were induced by heat. It is also possible that some of these chaperones are regulated by *ERF115*, connecting DNA damage, activation of QC cell division, and auxin signaling. However, further experiments need to be done to clarify this possibility.

Based on our data, we strongly believe that use of the TGRooZ can improve our understanding of how plants respond, as entire organisms (shoots and roots), to heat stress and also improve the translation of laboratory data to field trials.

Heat stress affects stem cell activity

Plant root growth and development rely on a coordinated balance between cell division and differentiation. In the RAM, the stem cell niche supplies new cells to the root pool by continuous cell divisions to sustain growth. This stem cell niche is organized and maintained by a small group of cells called the QC that rarely divide (Dolan et al., 1993; van den Berg et al., 1997). The QC cells can replenish the stem cell niche when its cells are damaged or prematurely differentiated (Cruz-Ramírez et al., 2013). It was shown that *ERF115* functions in slowing QC cell division and ensures the longevity of the stem cell niche (Heyman et al., 2013), whereas cytokinin activates the cell division of QC cells in Arabidopsis roots (Zhang et al., 2013). In dark-grown roots exposed to excessive high temperature, *ERF115* expression is induced in QC, pericycle, and vascular cells, probably to prevent their collapse. Interestingly, if *ERF115* is ectopically over-expressed, the resulting plants do not fully recover root growth in the temperature gradient. A possible explanation for this effect could be that $ERF115^{OE}$ roots are temporarily exposed to high temperature in the upper part of the gradient, activating a stress-response system that, combined with an over-accumulation of ERF115, delays root growth. In addition, acute high temperature has strong effects on the root meristem of *ERF115* over-expressing plants, likely because of a constitutive over-response of *ERF115* signaling. It should be noted that, as a general trend, stronger propidium iodide staining was observed in *erf115* mutant than in 32SR WT seedlings, suggesting a higher rate of cell death in the meristematic area. The response to cell death and DNA damage is controlled by the SOG1 pathway (Bourbousse et al., 2018), which seems to control the transcription of *ERF115*, as well as *ANAC085* and *HSP70.2*, among others. These data suggest that high temperatures in the root meristem lead to cell death and/or DNA damage, inducing a rescue system that involves *ERF115*, *ANAC085*, and *HSP*. In this work, we show that several *ERF* transcription factors with functions in cytokinin signaling (Rashotte et al., 2006) are activated, but

only by the effect of high homogeneous temperatures (Supplementary Table 1G), suggesting that they might regulate QC cell division via ERF-cytokinin signaling (Zhang et al., 2013). ERF members related to ethylene signaling such as *ERF109* or *ERF114* (Kong et al., 2018) are repressed and upregulated, respectively, indicating a complex balance of ERF family members in response to heat. The maintenance of the stem cell subpopulation to replace damaged stem cells might represent a general mechanism for ensuring a functional stem cell niche under stress conditions, including extremely high temperatures (Ubogoeva et al., 2021). Stress signals activate QC cell proliferation with the aim of restoring root growth in the case of major damage. In rice, the *ERF115* ortholog is involved in heat and drought stress tolerance (Park et al., 2021). In recent years, an emerging role for plant ERF transcription factors in stress responses is becoming evident. In our transcriptomic data, we identified a greater number of ERF factors (Supplemental Table 1) differentially expressed in response to heat stress than previously indicated (Heyman et al., 2018). Our data suggest that *ERF115* is needed to sustain root growth in response to high temperatures and also to maintain meristem activity when the shoot is subjected to high temperatures, as *erf115* seedlings do not fully recover root meristem size to control levels when grown in the TGRooZ. Similarly, root growth does not fully recover in the *hsfa2* mutant grown in a root temperature gradient. Interestingly, a gene regulatory network for cellular reprogramming in plant regeneration shows that *ERF115* and *HSFA2* are co-regulated by similar transcription factors of the LOB/AS2 family (Ikeuchi et al., 2018), suggesting an interconnection between these two genes. *HSFA2* regulates the expression of HSPs and is required for the acquisition and extension of plant thermotolerance (Charng et al., 2006). Analyses of mutants of individual members of the HSP 70 (HSP70.2) family did not reveal morphological phenotypes (Leng et al., 2017). Under these conditions, heat stress decreases root growth and the number of LRs formed in 32TGRooZ *hsp70.2* mutant seedlings, indicating that this gene, similar to *HSFA2*, might connect shoot heat stress responses with root development. Using the TGRooZ, we have been able to identify new genes that function in root responses to heat stress. This has been possible because the root responses are not blocked by the excessively high temperature that is normally used in heat stress experiments, supporting the idea that plants under heat stress should be cultivated with the root system in a temperature gradient like that observed in the field.

Heat stress affects plant Pi nutrition

Different transcriptomic analyses have pointed out the interconnection between high temperature and Pi starvation responses (Pacak et al., 2016; Giri et al., 2017). Here, we show that high temperatures affect several genes related to Pi starvation and decrease the level of Pi in roots and shoots. The KIG collection of genes involved in plant ionome composition was significantly regulated by temperature in shoots and roots. Interestingly, two of the main Pi starvation regulators were downregulated in accordance with our data, showing an increase in Pi nutrition pathways and accumulation (Whitt et al., 2020). Remarkably, a significant number of these KIG genes were also regulated by temperature in the root and shoot. Mutation of *PHO2* increases the Pi level in the shoot by increasing the activity of the PHO1 transporter (Bari et al., 2006; Pacak et al., 2016). Mutations of *PHR1* and its homolog *PHL1*, key transcription factors that regulate the Pi starvation response, decrease the level of Pi in the shoot (Rouached et al., 2011). In response to high temperatures, *PHR1* and *PHO2* were downregulated, but levels of *PHO1*:*3* increased. However, contrary to our expectations, these 32SR seedlings accumulated a lower Pi level in their shoots. It is possible that high temperature alters the Pi balance and that seedlings therefore respond by regulating a set of Pi-related genes to equilibrate Pi homeostasis during heat stress. As high temperatures decrease Pi nutrition, it is possible that this decrease could be one of the major limiting factors affecting plant growth. This idea is supported by the fact that *pho2* accumulates a greater Pi content in response to heat, but only when plants are grown under TGRooZ conditions. Interestingly, this greater accumulation correlates with an increase in *pho2* biomass production. Our results indicate a close correlation between heat stress and Pi nutrition; therefore, the TGRooZ will be useful for analyzing plant nutritional status during climate change.

Microbiome assembly and plant growth are influenced by soil temperature

Nutrient availability and plant productivity are determined to a large extent by soil properties and the soil microbial community inhabiting the root. The soil microbiota can be affected by diverse soil factors such as nutrient content, pH, and soil texture (Chaparro et al., 2012). The effects of climate change factors such as elevated CO_2, drought, and higher temperature on beneficial plant–microbe interactions are increasingly being explored. For example, soil temperature affects the recruitment of microbiota by plant roots (Compant et al., 2010; Rousk et al., 2012), and increased soil temperature may help roots to select microbial species that possess heat tolerance mechanisms and high growth rates rather than temperature-sensitive and slow-growing microbes (van der Voort et al., 2016). This community disturbance might lead to changes in plant growth, pathogen protection, or abiotic stress responses (Hariprasad et al., 2021; Vogel et al., 2021).

A hypothetical model based on the responses of microbial communities to temperature sensitivity suggests that the growth of bacterial and fungal soil communities tends to increase under moderately high temperatures; however, microbial diversity decreases significantly when the soil is exposed to a continuous high temperature (Nottingham et al., 2019). This decrease in diversity was also observed when soil was incubated at 35°C for a long period of time (Lin et al., 2017); during a wildfire, which increases the soi temperature to abnormally high levels, leading to a decrease in microbial activity and major changes in microbial communities (Ferrenberg et al., 2013; Jolly et al., 2015); and during solarization (soil heating) to sterilize soil, a procedure widely used in agriculture to eliminate or decrease the soil microbiota (Katan and Gamliel, 2014). Here, our data clearly show that plants exposed to shoot/root homogenous high temperature accommodate a different rhizosphere- and root-associated microbiome than plants grown at a lower temperature or with a high shoot temperature of 36°C and roots in a temperature gradient, conditions that replicate soil changes in natural ecosystems. We found that homogeneous

high temperature changes the beta diversity of both the rhizosphere and the root-associated microbiome, as well as mineral nutrient accumulation in leaves.

In general, the microbiome characteristics of tomato plants under optimal temperature described in this manuscript replicated general observations found in tomato plants in other published papers (Lee et al., 2021a). It is well established that plants under stress can change the root microbiome composition, enhancing the reproduction of beneficial microbes that represent an advantage for plant fitness. As high temperature can modulate the plant immune system (Huot et al., 2017), we speculate that part of the tomato plant's response to high temperature might overlap with the activation of plant defense, with the plant sensing an increase in temperature partially as a pathogen attack. In line with this hypothesis, the abundance of Actinobacteria was higher in the rhizosphere of tomato plants that were tolerant to bacterial wilt disease than in that of susceptible plants, whereas the abundance of Proteobacteria was lower (Huot et al., 2017). Therefore, changes in Actinobacteria and Proteobacteria observed in 36SR tomato plants might be associated with the plant stress response and specifically with changes in the activation of plant immune system components. Thus, changes in the ratio of Actinobacteria to Proteobacteria indicate that high temperatures alter the capacity of the root to recruit a typical microbiota. This observation supports the idea that the root might function as a sensing hub for abiotic and biotic stresses and that high soil temperature, but not the gradient of temperature in the root, disturbs the equilibrium and affects root functionality. Nevertheless, this hypothesis must be tested in future analyses.

Taken together, our results demonstrate that over-warming the soil compromises root function, which in turn may decrease plant capacity to cope with environmental changes. We envision that the system provided here, TGRooZ, will help with the design of new experiments aimed at mitigating the coming heat waves caused by climate change. In addition, our approach will be helpful for studying root growth and adaptation of soil-grown plants in response to heat, a trait that has been understudied in the last decades and that will definitely result in improved harvests and food security.

METHODS

Plant material

In this work, we used Arabidopsis ecotype Columbia and the tomato variety 'Moneymaker.' We used SKP2Bp:GUS (Manzano et al., 2012) as a marker for LRP, as well as the reporter line WOX5:GFP (Sarkar et al., 2007) and the marker line *CYCB1;1:CYCB1;1-GFP* (Ubeda-Tomas et al., 2009). The Arabidopsis mutants were obtained from the NASC stock center with the following code numbers: SALK_208662 (NAC085 AT5G14490); SALK_008978 (HSFA2 AT2G26150); SALK_085076 (HSP70.2 AT5G02490); and SALK_075596 (HSP90.1 AT5G52640).

The erf115, *ERF115*^{OE}, and *ERF115*^{SDRX} lines were described in (Heyman et al., 2013; Canher et al., 2021). The *pho2* (Aung et al., 2006), *phr1 phl1* (Bustos et al., 2010), *axr1-12* (Lincoln et al., 1990), and *tir1-1* (Ruegger et al., 1998) mutants were used to analyze the effect of auxin signaling or Pi starvation responses on high temperature responses.

Growing conditions

Arabidopsis seedlings were germinated in half-strength Murashige and Skoog (MS) medium (MS1/2) with vitamins plus 1% sucrose, 1% Difco Agar, and 0.05% MES (pH 5.8) using the D-Root device to prevent root illumination (Silva-Navas et al., 2015) or in the TGRooZ device (Supplemental Figure 1) to generate a temperature gradient. The top of the TGRooZ device was closed with an iron cover that has rectangular holes to fit a 12 × 12-cm square *in vitro* plate or holes for a 30 × 40-cm zip bag containing a germination paper. The plant growth chamber was set to 22°C (standard) or 32°C (heat stress) for Arabidopsis and 26°C and 36°C for tomato using the germination paper system (Supplemental Figure 3). To generate the temperature gradient, the TGRooZ refrigerated liquid was cooled to 13°C for Arabidopsis or 10.5°C for tomato. Seedlings were germinated in MS1/2 for 4 days at 22°C and then transferred to 22°C (22SR seedlings), 32°C (32SR seedlings), or 32°C with a temperature gradient (32TGRooZ) for 6 more days. To analyze heat stress in tomato grown in soil, pots containing tomato plants were placed in the adapted TGRooZ (Supplemental Figure 1), and the growth chambers were set to 22°C or 36°C. For the 36TGRooZ condition, to generate the gradient the refrigerant liquid in the base of the modified TGRooZ (Supplemental Figure 1D) was cooled at 10°C. Tomato seedlings were germinated in vermiculite at 22°C, and tomato seedlings of similar size were transplanted to soil. They were grown at 22°C for 2 more days and then moved to 22°C (22SR seedlings), 36ºC (36SR seedlings), or 36°C with a temperature gradient (36TGRooZ seedlings) for 3 more weeks at a relative humidity of 40%. Plants were grown under a 16-h light/8-h dark photoperiod with a light fluency rate of 130 μM m^{-1} sec^{-1}.

Root morphological analyses

The 22SR, 32SR, and 32TRGooZ seedlings were grown as described above. They were scanned at a high resolution with an Epson 600V scanner, and root and hypocotyl length and cotyledon epinasty angle were quantified using Fiji software. To quantify LRP, SKP2Bp:GUS seedlings were stained for GUS activity as described by Silva-Navas (Silva-Navas et al., 2015), and GUS-stained LRP were quantified using a Leica Z9 stereomicroscope.

Mitotic cell quantification and root meristem size

The 22SR, 32SR, and 32TRGooZ Arabidopsis seedlings were grown as described above using *in vitro* plates. Root meristem size was quantified from confocal images taken with a Leica Z8 microscope of the RAM stained with propidium iodide as described by González-García et al. (2011). PI and GFP were detected with a band-pass 570–670-nm filter and 500–545-nm filter, respectively, and observed under a confocal microscope (Leica TCS-SP8). Size was calculated based on the number of meristematic cortical cells and/or the distance from the QC to the last meristematic cell. The end of the meristem zone was taken as the point where a meristematic cortical cell doubled in size from the previous one. Mitotic cell numbers were quantified using the *CYCB1;1:CYCB1;1-GFP* marker line (Ubeda-Tomas et al., 2009). The number of fluorescent cells was quantified through all stacks.

Root length, number of LRs, hypocotyl length, leaf epinasty angle, and root meristem size in Arabidopsis were assessed in at least three independent experiments. Roots were scanned and root length measured with ImageJ software (http://rsb.info.nih.gov/ij/). For comparisons, significance was analyzed by ANOVA and Tukey's honestly significant difference post-test using a p value <0.05 in all cases.

Transcriptomic analyses

To carry out the transcriptomic analyses, total RNA was extracted from roots and shoots of Arabidopsis seedlings that were germinated for 4 days at 22°C and then transferred for 7 more days to 22°C (22SR), 32°C (32SR), or 32°C with a temperature gradient in the root zone (32TGRooZ) (32°C at the top of the plate and 18°C at the bottom). In the

case of 22°C, we had only two replicates because the third degraded during processing. Library construction and RNA sequencing were performed by Beijing Genomics Institute (BGI-Shenzhen), and 30 M reads were obtained (100 PE; average quality 96%). Approximately 20 μg total RNA was subjected to poly-A^+RNA isolation by oligo-dT chromatography, followed by RNA fragmentation. Fragmented RNA was converted to double-stranded cDNA using random hexamer primers followed by end repair, 3′ end adenylation, and adapter ligation. cDNA fragments were selected by agarose gel extraction and enriched by PCR amplification. The library was loaded onto an Illumina HiSeq 2000 instrument for paired-end sequencing (average raw read length, 100 bp).

Before assembly, FastQC (Andrews, 2010) (v0.11.9) was used to obtain information about the quality of the sequencing data. This information was used for the initial filtering of sequences by Trimmomatic (v0.36) (Bolger et al., 2014). For each sample, RNA sequencing (RNA-seq) raw reads (paired-end, 100 bp) were trimmed to remove potential Illumina adaptor contamination, followed by read trimming and clipping of low-quality bases. The remaining reads were aligned to the *A. thaliana* TAIR10 reference genome using the Araport11 annotation (Cheng et al., 2017) with the STAR aligner (v2.5.3a) (Dobin et al., 2013) and the following command-line parameters: –outFilterMultimapNmax 20 –alignSJoverhangMin 8 –alignSJDBoverhangMin 8 –outFilterMismatchNmax 8 –alignIntronMin 35 –alignMatesGapMax 100 000 –alignIntronMax 20 000. Based on the RNA-seq mapped reads and the Araport11 annotation, HTSeq (v1.99.2) (Anders and Huber, 2010) with the intersection 'union' option was used to generate the read counts per gene. Normalization and statistical analyses of differential gene expression were performed with the DESeq2 Bioconductor package in R (Anders and Huber, 2010; Love et al., 2014). A multiple-testing-corrected p value (q value) (Benjamini and Hochberg, 1995) of 0.05 was used. Differentially expressed genes were defined as those genes with a corrected p value of <0.05 and a $\log_2$(fold-change) >0.8 or <–0.8.

Gene ontology and statistical analyses

Gene ontology analyses were performed using the Metascape tool (https://metascape.org/gp/index.html#/main/step1) with the following parameters: minimum overlapping of 3, p value cutoff of 0.05, and minimum enrichment of 1.5. The overall data were statistically analyzed using GraphPad5 software. Comparisons between two groups were made with Student's t-test, and multigroup comparisons were made using one-way ANOVA followed by Tukey's test. A p value of less than 0.05 was considered statistically significant, and significant differences are indicated by different letters.

Free Pi quantification

Arabidopsis plants were germinated in MS1/2 medium for 4 days at 22°C and then transferred to 22°C (22SR), 32°C (32SR), or 32°C with a temperature gradient in the root zone (32TGRooZ) for 6 moredays. Roots and shoots were collected separately, and inorganic Pi was quantified as described previously (Ames, 1966). Free Pi was expressedper plant or per mg. For every plate analyzed, the total amount of Pi (nmoles) was divided by the number of plants in the plate or divided by the total fresh weight (n = 6 plates).

For the *phr1 phl1* and *pho2* mutants, free Pi (nmoles of Pi) and fresh weight (mg) wereexpressed per plant. Afterwards, shoot and root fresh weights or Pi levels of seedlings grown at different temperatures were standardized with respect to those of plants grown at 22°C.

DATA AVAILABILITY

RNA-Seq data are deposited in the GEO Data Bank (GSE214280).

SUPPLEMENTAL INFORMATION

Supplemental information is available at *Plant Communications Online*.

FUNDING

The authors thank Malcolm Bennet for *CYCB1;1:CYCB1;1-GFP*, Lieven De Veylder for the *erf115* mutant (SALK_021981), *ERF115*^{SDRX}, *ERF115*^{OE}, and pERF115:NLS-GUS/GFP (Heyman et al., 2013), and Javier Paz Ares for the *phr1 phl1* double mutant and *pho2*. We also thank the CBGP's Plant Facility Service and Bioinformatic Unit for help with plant growth, treatments, and bioinformatics analyses. This research was supported by grants from the Spanish Government BIO2017-82209-R and PID2020-113479RB-I00 granted by MCIN/AEI/10.13039/501100011033/ to J.C.P and by the "Severo Ochoa Program for Centres of Excellence in R&D" from the Agencia Estatal de Investigación of Spain (grant SEV-2016-0672; 2017–2021) to the C.B.G.P. M.P.G.G. is supported by a postdoctoral contract associated with the "Severo Ochoa Program" and a UPM talent attraction contract. C.M.C. and M.S.-B. are supported by a predoctoral fellowship (BES-2017-082152 and PRE2019-088076 respectively) associated with the Severo Ochoa Program. V.B.G. is supported by the Ministry of Universities (predoctoral fellowship FPU20/07 453). G.C. was supported by the Biotechnology and Biological Sciences Research Council and the National Science Foundation (BBSRC-NSF), grant no. BB/V011294/1, and the Leverhulme Trust, grant no. RPG-2019-337.

AUTHOR CONTRIBUTIONS

M.P.G.G., C.M.C., A.L., B.S., S.N.N., V.B., and M.S. performed the experiments, and M.P.G.G., C.M.C., G.C., and J.C.P. planned and designed the research. I.S.-G., G.C., E.C., and J.C.P. analyzed the data. M.P.G.G., E.C., I.S.-G., G.C., and J.C.P. wrote and edited the manuscript.

ACKNOWLEDGMENTS

No conflict of interest declared.

Received: July 19, 2022
Revised: December 22, 2022
Accepted: December 29, 2022
Published: December 30, 2022

REFERENCES

Ai, H., Bellstaedt, J., Bartusch, K.S., Eschen-Lippold, L., Babben, S., Balcke, G.U., Tissier, A., Hause, B., Andersen, T.G., Delker, C., et al. (2022). Auxin-dependent acceleration of cell division rates regulates root growth at elevated temperature. Preprint at bioRxiv. https://doi.org/10.1101/2022.06.22.497127.

Ames, B.N. (1966). Assay of inorganic phosphate, total phosphate and phosphatases. In In Methods in Enzymology (Academic Press), pp. 115–118. https://doi.org/10.1016/0076-6879(66)08014-5.

Anders, S., and Huber, W. (2010). Differential expression analysis for sequence count data. Genome Biol. **11**:R106. https://doi.org/10.1186/gb-2010-11-10-r106.

Andrews, S. (2010). FastQC: A Quality Control Tool for High Throughput Sequence Data. http://www.bioinformatics.babraham.ac.uk/projects/fastqc.

Aung, K., Lin, S.I., Wu, C.C., Huang, Y.T., Su, C.L., and Chiou, T.J. (2006). pho2, a phosphate overaccumulator, is caused by a nonsense mutation in a microRNA399 target gene. Plant Physiol. **141**:1000–1011. https://doi.org/10.1104/pp.106.078063.

Bari, R., Datt Pant, B., Stitt, M., and Scheible, W.R. (2006). PHO2, microRNA399, and PHR1 define a phosphate-signaling pathway in plants. Plant Physiol. **141**:988–999. https://doi.org/10.1104/pp.106.079707.

Baskin, T., Betzner, A., Hoggart, R., Cork, A., and Williamson, R. (1992). Root morphology mutants in <I>Arabidopsis thaliana</I&gt. Functional Plant Biol. **19**:427–437. https://doi.org/10.1071/PP9920427.

Bellstaedt, J., Trenner, J., Lippmann, R., Poeschl, Y., Zhang, X., Friml, J., Quint, M., and Delker, C. (2019). A mobile auxin signal connects temperature sensing in cotyledons with growth responses

in hypocotyls. Plant Physiol. **180**:757–766. https://doi.org/10.1104/pp.18.01377.

Benjamini, Y., and Hochberg, Y. (1995). Controlling the false discovery rate: a practical and powerful approach to multiple testing. J. Roy. Stat. Soc. B **57**:289–300.

Bhattacharya, A. (2019). Chapter 1 - effect of high-temperature stress on crop productivity. In In Effect of High Temperature on Crop Productivity and Metabolism of Macro Molecules, A. Bhattacharya, ed. (Academic Press), pp. 1–114. https://doi.org/10.1016/B978-0-12-817562-0.00001-X.

Bolger, A.M., Lohse, M., and Usadel, B. (2014). Trimmomatic: a flexible trimmer for Illumina sequence data. Bioinformatics **30**:2114–2120. https://doi.org/10.1093/bioinformatics/btu170.

Bourbousse, C., Vegesna, N., and Law, J.A. (2018). SOG1 activator and MYB3R repressors regulate a complex DNA damage network in <i>Arabidopsis</i&gt. Proc. Natl. Acad. Sci. USA. **115**:E12453–E12462. https://doi.org/10.1073/pnas.1810582115.

Brunetti, C., Lamb, J., Wielandt, S., Uhlemann, S., Shirley, I., McClure, P., and Dafflon, B. (2021). Estimation of depth-resolved profiles of soil thermal diffusivity from temperature time series and uncertainty quantification. Earth Surf. Dynam. Discuss. **2021**:1–25. https://doi.org/10.5194/esurf-2021-68.

Bustos, R., Castrillo, G., Linhares, F., Puga, M.I., Rubio, V., Pérez-Pérez, J., Solano, R., Leyva, A., and Paz-Ares, J. (2010). A central regulatory system largely controls transcriptional activation and repression responses to phosphate starvation in Arabidopsis. PLoS Genet. **6**:e1001102. https://doi.org/10.1371/journal.pgen.1001102.

Calleja-Cabrera, J., Boter, M., Oñate-Sánchez, L., and Pernas, M. (2020). Root growth adaptation to climate change in crops. Front. Plant Sci. **11**:544. https://doi.org/10.3389/fpls.2020.00544.

Canher, B., Lanssens, F., Zhang, A., Bisht, A., Mazumdar, S., Heyman, J., Augstein, F., Wolf, S., Carlsbecker, A., Melnyk, C.W., et al. (2021). The regeneration factors ERF114 and ERF115 act as transducers of mechanical cues to developmental pathways. Preprint at bioRxiv. https://doi.org/10.1101/2021.11.29.470368.

Castrillo, G., Teixeira, P.J.P.L., Paredes, S.H., Law, T.F., de Lorenzo, L., Feltcher, M.E., Finkel, O.M., Breakfield, N.W., Mieczkowski, P., Jones, C.D., et al. (2017). Root microbiota drive direct integration of phosphate stress and immunity. Nature **543**:513–518. https://doi.org/10.1038/nature21417.

Chaparro, J.M., Sheflin, A.M., Manter, D.K., and Vivanco, J.M. (2012). Manipulating the soil microbiome to increase soil health and plant fertility. Biol. Fertil. Soils **48**:489–499. https://doi.org/10.1007/s00374-012-0691-4.

Charng, Y.-y., Liu, H.-c., Liu, N.-y., Chi, W.-t., Wang, C.-n., Chang, S.-h., and Wang, T.-t. (2006). A heat-inducible transcription factor, HsfA2, is required for extension of acquired thermotolerance in Arabidopsis. Plant Physiol. **143**:251–262. https://doi.org/10.1104/pp.106.091322.

Chen, S., and Li, H. (2017). Heat stress regulates the expression of genes at transcriptional and post-transcriptional levels, revealed by RNA-seq in brachypodium distachyon. Front. Plant Sci. **7**. https://doi.org/10.3389/fpls.2016.02067.

Cheng, C.Y., Krishnakumar, V., Chan, A.P., Thibaud-Nissen, F., Schobel, S., and Town, C.D. (2017). Araport11: a complete reannotation of the Arabidopsis thaliana reference genome. Plant J. **89**:789–804. https://doi.org/10.1111/tpj.13415.

Compant, S., van der Heijden, M.G.A., and Sessitsch, A. (2010). Climate change effects on beneficial plant-microorganism interactions. FEMS Microbiol. Ecol. **73**:197–214. https://doi.org/10.1111/j.1574-6941.2010.00900.x.

Cruz-Ramírez, A., Díaz-Triviño, S., Wachsman, G., Du, Y., Arteága-Vázquez, M., Zhang, H., Benjamins, R., Blilou, I., Neef, A.B., Chandler, V., et al. (2013). A SCARECROW-RETINOBLASTOMA protein network controls protective quiescence in the Arabidopsis root stem cell organizer. PLoS Biol. **11**:e1001724. https://doi.org/10.1371/journal.pbio.1001724.

de la Fuente Cantó, C., Simonin, M., King, E., Moulin, L., Bennett, M.J., Castrillo, G., and Laplaze, L. (2020). An extended root phenotype: the rhizosphere, its formation and impacts on plant fitness. Plant J. **103**:951–964. https://doi.org/10.1111/tpj.14781.

Dobin, A., Davis, C.A., Schlesinger, F., Drenkow, J., Zaleski, C., Jha, S., Batut, P., Chaisson, M., and Gingeras, T.R. (2013). STAR: ultrafast universal RNA-seq aligner. Bioinformatics **29**:15–21. https://doi.org/10.1093/bioinformatics/bts635.

Dolan, L., Janmaat, K., Willemsen, V., Linstead, P., Poethig, S., Roberts, K., and Scheres, B. (1993). Cellular organisation of the Arabidopsis thaliana root. Development **119**:71–84.

Elias, E.A., Cichota, R., Torriani, H.H., and de Jong van Lier, Q. (2004). Analytical soil–temperature model. Soil Sci. Soc. Am. J. **68**:784–788. https://doi.org/10.2136/sssaj2004.7840.

Estravis-Barcala, M., Heer, K., Marchelli, P., Ziegenhagen, B., Arana, M.V., and Bellora, N. (2021). Deciphering the transcriptomic regulation of heat stress responses in Nothofagus pumilio. PLoS One **16**:e0246615. https://doi.org/10.1371/journal.pone.0246615.

Fahad, S., Bajwa, A.A., Nazir, U., Anjum, S.A., Farooq, A., Zohaib, A., Sadia, S., Nasim, W., Adkins, S., Saud, S., et al. (2017). Crop production under drought and heat stress: plant responses and management options. Front. Plant Sci. **8**:1147. https://doi.org/10.3389/fpls.2017.01147.

Ferrenberg, S., O'Neill, S.P., Knelman, J.E., Todd, B., Duggan, S., Bradley, D., Robinson, T., Schmidt, S.K., Townsend, A.R., Williams, M.W., et al. (2013). Changes in assembly processes in soil bacterial communities following a wildfire disturbance. ISME J. **7**:1102–1111. https://doi.org/10.1038/ismej.2013.11.

Finkel, O.M., Salas-González, I., Castrillo, G., Spaepen, S., Law, T.F., Teixeira, P.J.P.L., Jones, C.D., and Dangl, J.L. (2019). The effects of soil phosphorus content on plant microbiota are driven by the plant phosphate starvation response. PLoS Biol. **17**:e3000534. https://doi.org/10.1371/journal.pbio.3000534.

Friedrich, T., Oberkofler, V., Trindade, I., Altmann, S., Brzezinka, K., Lämke, J., Gorka, M., Kappel, C., Sokolowska, E., Skirycz, A., et al. (2021). Heteromeric HSFA2/HSFA3 complexes drive transcriptional memory after heat stress in Arabidopsis. Nat. Commun. **12**:3426. https://doi.org/10.1038/s41467-021-23786-6.

Gaillochet, C., Burko, Y., Platre, M.P., Zhang, L., Simura, J., Willige, B.C., Kumar, S.V., Ljung, K., Chory, J., and Busch, W. (2020). HY5 and phytochrome activity modulate shoot-to-root coordination during thermomorphogenesis in Arabidopsis. Development **147**:dev192625. https://doi.org/10.1242/dev.192625.

Giri, A., Heckathorn, S., Mishra, S., and Krause, C. (2017). Heat stress decreases levels of nutrient-uptake and -assimilation proteins in tomato roots. Plants **6**:6. https://doi.org/10.3390/plants6010006.

Gomaa, N.H., Montesinos-Navarro, A., Alonso-Blanco, C., and Picó, F.X. (2011). Temporal variation in genetic diversity and effective population size of Mediterranean and subalpine Arabidopsis thaliana populations. Mol. Ecol. **20**:3540–3554. https://doi.org/10.1111/j.1365-294X.2011.05193.x.

González-García, M.P., Vilarrasa-Blasi, J., Zhiponova, M., Divol, F., Mora-García, S., Russinova, E., and Caño-Delgado, A.I. (2011). Brassinosteroids control meristem size by promoting cell cycle progression in Arabidopsis roots. Development **138**:849–859. https://doi.org/10.1242/dev.057331.

Gray, S.B., and Brady, S.M. (2016). Plant developmental responses to climate change. Dev. Biol. **419**:64–77. https://doi.org/10.1016/j.ydbio.2016.07.023.

Gray, W.M., Ostin, A., Sandberg, G., Romano, C.P., and Estelle, M. (1998). High temperature promotes auxin-mediated hypocotyl elongation in Arabidopsis. Proc. Natl. Acad. Sci. USA. **95**:7197–7202.

Hariprasad, P., Gowtham, H.G., and Gourav, C. (2021). Beneficial plant-associated bacteria modulate host hormonal system enhancing plant resistance toward abiotic stress. In In Biocontrol Agents and Secondary Metabolites, S. Jogaiah, ed. (Woodhead Publishing), pp. 113–151. https://doi.org/10.1016/B978-0-12-822919-4.00006-5.

Hasanuzzaman, M., Nahar, K., Alam, M.M., Roychowdhury, R., and Fujita, M. (2013). Physiological, biochemical, and molecular mechanisms of heat stress tolerance in plants. Int. J. Mol. Sci. **14**:9643–9684. https://doi.org/10.3390/ijms14059643.

Hatfield, J.L., and Prueger, J.H. (2015). Temperature extremes: effect on plant growth and development. Weather Clim. Extrem. **10**:4–10. https://doi.org/10.1016/j.wace.2015.08.001.

Heckathorn, S.A., Giri, A., Mishra, S., and Bista, D. (2013). Heat stress and roots. In In Climate Change and Plant Abiotic Stress Tolerance, pp. 109–136. https://doi.org/10.1002/9783527675265.ch05.

Heyman, J., Canher, B., Bisht, A., Christiaens, F., and De Veylder, L. (2018). Emerging role of the plant ERF transcription factors in coordinating wound defense responses and repair. J. Cell Sci. **131**. https://doi.org/10.1242/jcs.208215.

Heyman, J., Cools, T., Vandenbussche, F., Heyndrickx, K.S., Van Leene, J., Vercauteren, I., Vanderauwera, S., Vandepoele, K., De Jaeger, G., Van Der Straeten, D., et al. (2013). ERF115 controls root quiescent center cell division and stem cell replenishment. Science **342**:860–863. https://doi.org/10.1126/science.1240667.

Huang, B., Rachmilevitch, S., and Xu, J. (2012). Root carbon and protein metabolism associated with heat tolerance. J. Exp. Bot. **63**:3455–3465. https://doi.org/10.1093/jxb/ers003.

Huot, B., Castroverde, C.D.M., Velásquez, A.C., Hubbard, E., Pulman, J.A., Yao, J., Childs, K.L., Tsuda, K., Montgomery, B.L., and He, S.Y. (2017). Dual impact of elevated temperature on plant defence and bacterial virulence in Arabidopsis. Nat. Commun. **8**:1808. https://doi.org/10.1038/s41467-017-01674-2.

Ikeuchi, M., Shibata, M., Rymen, B., Iwase, A., Bågman, A.M., Watt, L., Coleman, D., Favero, D.S., Takahashi, T., Ahnert, S.E., et al. (2018). A gene regulatory network for cellular reprogramming in plant regeneration. Plant Cell Physiol. **59**:765–777. https://doi.org/10.1093/pcp/pcy013.

Jolly, W.M., Cochrane, M.A., Freeborn, P.H., Holden, Z.A., Brown, T.J., Williamson, G.J., and Bowman, D.M.J.S. (2015). Climate-induced variations in global wildfire danger from 1979 to 2013. Nat. Commun. **6**:7537. https://doi.org/10.1038/ncomms8537.

Katan, J., and Gamliel, A. (2014). Plant health management: soil solarization. In In Encyclopedia of Agriculture and Food Systems, N.K. Van Alfen, ed. (Oxford: Academic Press), pp. 460–471. https://doi.org/10.1016/B978-0-444-52512-3.00256-4.

Kong, X., Tian, H., Yu, Q., Zhang, F., Wang, R., Gao, S., Xu, W., Liu, J., Shani, E., Fu, C., et al. (2018). PHB3 maintains root stem cell niche identity through ROS-responsive AP2/ERF transcription factors in Arabidopsis. Cell Rep. **22**:1350–1363. https://doi.org/10.1016/j.celrep.2017.12.105.

Küpers, J.J., Oskam, L., and Pierik, R. (2020). Photoreceptors regulate plant developmental plasticity through auxin. Plants **9**:940. https://doi.org/10.3390/plants9080940.

Lahti, M., Aphalo, P.J., Finér, L., Ryyppö, A., Lehto, T., and Mannerkoski, H. (2005). Effects of soil temperature on shoot and root growth and nutrient uptake of 5-year-old Norway spruce seedlings. Tree Physiol. **25**:115–122. https://doi.org/10.1093/treephys/25.1.115.

Larkindale, J., and Vierling, E. (2008). Core genome responses involved in acclimation to high temperature. Plant Physiol. **146**:748–761. https://doi.org/10.1104/pp.107.112060.

Larkindale, J., Hall, J.D., Knight, M.R., and Vierling, E. (2005). Heat stress phenotypes of Arabidopsis mutants implicate multiple signaling pathways in the acquisition of thermotolerance. Plant Physiol. **138**:882–897. https://doi.org/10.1104/pp.105.062257.

Lee, S., Wang, W., and Huq, E. (2021b). Spatial regulation of thermomorphogenesis by HY5 and PIF4 in Arabidopsis. Nat. Commun. **12**:3656. https://doi.org/10.1038/s41467-021-24018-7.

Lee, S.-M., Kong, H.G., Song, G.C., and Ryu, C.-M. (2021a). Disruption of Firmicutes and Actinobacteria abundance in tomato rhizosphere causes the incidence of bacterial wilt disease. ISME J. **15**:330–347. https://doi.org/10.1038/s41396-020-00785-x.

Leng, L., Liang, Q., Jiang, J., Zhang, C., Hao, Y., Wang, X., and Su, W. (2017). A subclass of HSP70s regulate development and abiotic stress responses in Arabidopsis thaliana. J. Plant Res. **130**:349–363. https://doi.org/10.1007/s10265-016-0900-6.

Lin, Y.T., Jia, Z., Wang, D., and Chiu, C.Y. (2017). Effects of temperature on the composition and diversity of bacterial communities in bamboo soils at different elevations. Biogeosciences **14**:4879–4889. https://doi.org/10.5194/bg-14-4879-2017.

Lincoln, C., Britton, J.H., and Estelle, M. (1990). Growth and development of the axr1 mutants of Arabidopsis. Plant Cell **2**:1071–1080. https://doi.org/10.1105/tpc.2.11.10712/11/1071.

Liu, J., Liu, Y., Wang, S., Cui, Y., and Yan, D. (2022). Heat stress reduces root meristem size via induction of plasmodesmal callose accumulation inhibiting phloem unloading in Arabidopsis. Int. J. Mol. Sci. **23**. https://doi.org/10.3390/ijms23042063.

Liu, T.Y., Huang, T.K., Tseng, C.Y., Lai, Y.S., Lin, S.I., Lin, W.Y., Chen, J.W., and Chiou, T.J. (2012). PHO2-dependent degradation of PHO1 modulates phosphate homeostasis in Arabidopsis. Plant Cell **24**:2168–2183. https://doi.org/10.1105/tpc.112.096636.

Love, M.I., Huber, W., and Anders, S. (2014). Moderated estimation of fold change and dispersion for RNA-seq data with DESeq2. Genome Biol. **15**:550. https://doi.org/10.1186/s13059-014-0550-8.

Lynch, J., Marschner, P., and Rengel, Z. (2012). Chapter 13 - effect of internal and external factors on root growth and development. In In Marschner's Mineral Nutrition of Higher Plants, Third Edition, P. Marschner, ed. (San Diego: Academic Press), pp. 331–346. https://doi.org/10.1016/B978-0-12-384905-2.00013-3.

Manzano, C., Ramirez-Parra, E., Casimiro, I., Otero, S., Desvoyes, B., De Rybel, B., Beeckman, T., Casero, P., Gutierrez, C., and C Del Pozo, J. (2012). Auxin and epigenetic regulation of SKP2B, an F-box that represses lateral root formation. Plant Physiol. **160**:749–762. https://doi.org/10.1104/pp.112.198341.

Michaletz, S.T., Weiser, M.D., Zhou, J., Kaspari, M., Helliker, B.R., and Enquist, B.J. (2015). Plant thermoregulation: energetics, trait–environment interactions, and carbon economics. Trends Ecol. Evol. **30**:714–724. https://doi.org/10.1016/j.tree.2015.09.006.

Miller, S., Chua, K., Coggins, J., and Mohtadi, H. (2021). Heat waves, climate change, and economic output. J. Eur. Econ. Assoc. **19**:2658–2694. https://doi.org/10.1093/jeea/jvab009.

Nagel, K.A., Kastenholz, B., Jahnke, S., van Dusschoten, D., Aach, T., Mühlich, M., Truhn, D., Scharr, H., Terjung, S., Walter, A., et al. (2009). Temperature responses of roots: impact on growth, root system architecture and implications for phenotyping. Funct. Plant Biol. **36**:947–959. https://doi.org/10.1071/fp09184.

Nottingham, A.T., Bååth, E., Reischke, S., Salinas, N., and Meir, P. (2019). Adaptation of soil microbial growth to temperature: using a

tropical elevation gradient to predict future changes. Glob. Chang. Biol. **25**:827–838. https://doi.org/10.1111/gcb.14502.

onwuka, B. (2018). Effects of soil temperature on some soil properties and plant growth. Advances in Plants & Agriculture Research **8**. https://doi.org/10.15406/apar.2018.08.00288.

Pacak, A., Barciszewska-Pacak, M., Swida-Barteczka, A., Kruszka, K., Sega, P., Milanowska, K., Jakobsen, I., Jarmolowski, A., and Szweykowska-Kulinska, Z. (2016). Heat stress affects pi-related genes expression and inorganic phosphate deposition/accumulation in barley. Front. Plant Sci. **7**:926. https://doi.org/10.3389/fpls.2016.00926.

Park, S.-I., Kwon, H.J., Cho, M.H., Song, J.S., Kim, B.-G., Baek, J., Kim, S.L., Ji, H., Kwon, T.-R., Kim, K.-H., et al. (2021). The OsERF115/AP2EREBP110 transcription factor is involved in the multiple stress tolerance to heat and drought in rice plants. Int. J. Mol. Sci. **22**:7181.

Pei, X., Zhang, Y., Zhu, L., Zhao, D., Lu, Y., and Zheng, J. (2021). Physiological and transcriptomic analyses characterized high temperature stress response mechanisms in Sorbus pohuashanensis. Sci. Rep. **11**:10117. https://doi.org/10.1038/s41598-021-89418-7.

Powers, S.K., and Strader, L.C. (2020). Regulation of auxin transcriptional responses. Dev. Dyn. **249**:483–495. https://doi.org/10.1002/dvdy.139.

Qi, F., and Zhang, F. (2020). Cell cycle regulation in the plant response to stress. Front. Plant Sci. **10**:1765. https://doi.org/10.3389/fpls.2019.01765.

Rashotte, A.M., Mason, M.G., Hutchison, C.E., Ferreira, F.J., Schaller, G.E., and Kieber, J.J. (2006). A subset of Arabidopsis AP2 transcription factors mediates cytokinin responses in concert with a two-component pathway. Proc. Natl. Acad. Sci. USA. **103**:11081–11085. https://doi.org/10.1073/pnas.0602038103.

Ren, H., and Gray, W.M. (2015). SAUR proteins as effectors of hormonal and environmental signals in plant growth. Mol. Plant **8**:1153–1164. https://doi.org/10.1016/j.molp.2015.05.003.

Rouached, H., Secco, D., Arpat, B., and Poirier, Y. (2011). The transcription factor PHR1 plays a key role in the regulation of sulfate shoot-to-root flux upon phosphate starvation in Arabidopsis. BMC Plant Biol. **11**:19. https://doi.org/10.1186/1471-2229-11-19.

Rousk, J., Frey, S.D., and Bååth, E. (2012). Temperature adaptation of bacterial communities in experimentally warmed forest soils. Glob. Chang. Biol. **18**:3252–3258. https://doi.org/10.1111/j.1365-2486.2012.02764.x.

Ruegger, M., Dewey, E., Gray, W.M., Hobbie, L., Turner, J., and Estelle, M. (1998). The TIR1 protein of Arabidopsis functions in auxin response and is related to human SKP2 and yeast grr1p. Genes Dev. **12**:198–207.

Sabri, N.S.A., Zakaria, Z., Mohamad, S.E., Jaafar, A.B., and Hara, H. (2018). Importance of soil temperature for the growth of temperate crops under a tropical climate and functional role of soil microbial diversity. Microbes Environ. **33**:144–150. https://doi.org/10.1264/jsme2.ME17181.

Sarkar, A.K., Luijten, M., Miyashima, S., Lenhard, M., Hashimoto, T., Nakajima, K., Scheres, B., Heidstra, R., and Laux, T. (2007). Conserved factors regulate signalling in Arabidopsis thaliana shoot and root stem cell organizers. Nature **446**:811–814. https://doi.org/10.1038/nature05703.

Schramm, F., Ganguli, A., Kiehlmann, E., Englich, G., Walch, D., and von Koskull-Döring, P. (2006). The heat stress transcription factor HsfA2 serves as a regulatory amplifier of a subset of genes in the heat stress response in Arabidopsis. Plant Mol. Biol. **60**:759–772. https://doi.org/10.1007/s11103-005-5750-x.

Silva-Navas, J., Conesa, C.M., Saez, A., Navarro-Neila, S., Garcia-Mina, J.M., Zamarreño, A.M., Baigorri, R., Swarup, R., and Del Pozo, J.C. (2019). Role of cis-zeatin in root responses to phosphate starvation. New Phytol. **224**:242–257. https://doi.org/10.1111/nph.16020.

Silva-Navas, J., Moreno-Risueno, M.A., Manzano, C., Pallero-Baena, M., Navarro-Neila, S., Téllez-Robledo, B., Garcia-Mina, J.M., Baigorri, R., Gallego, F.J., and del Pozo, J.C. (2015). D-Root: a system to cultivate plants with the root in darkness or under different light conditions. Plant J. **84**:244–255. https://doi.org/10.1111/tpj.12998.

Singh, S.K., Reddy, V.R., Fleisher, D.H., and Timlin, D.J. (2018). Phosphorus nutrition affects temperature response of soybean growth and canopy photosynthesis. Front. Plant Sci. **9**. https://doi.org/10.3389/fpls.2018.01116.

Smith, K.A. (2000). Soil and Environmental Analysis: Physical Methods, Revised, and Expanded, 2nd ed. (CRC Press). https://doi.org/10.1201/9780203908600.

Sriden, N., and Charoensawan, V. (2022). Large-scale comparative transcriptomic analysis of temperature-responsive genes in Arabidopsis thaliana. Plant Mol. Biol. **110**:425–443. https://doi.org/10.1007/s11103-021-01223-y.

Stortenbeker, N., and Bemer, M. (2018). The SAUR gene family: the plant's toolbox for adaptation of growth and development. J. Exp. Bot. **70**:17–27. https://doi.org/10.1093/jxb/ery332.

Sun, J., Qi, L., Li, Y., Chu, J., and Li, C. (2012). PIF4–Mediated activation of YUCCA8 expression integrates temperature into the auxin pathway in regulating Arabidopsis hypocotyl growth. PLoS Genet. **8**:e1002594. https://doi.org/10.1371/journal.pgen.1002594.

Takahashi, N., Ogita, N., Takahashi, T., Taniguchi, S., Tanaka, M., Seki, M., and Umeda, M. (2019). A regulatory module controlling stress-induced cell cycle arrest in Arabidopsis. Elife **8**:e43944. https://doi.org/10.7554/eLife.43944.

Tivendale, N.D., and Millar, A.H. (2022). How is auxin linked with cellular energy pathways to promote growth? New Phytol. **233**:2397–2404. https://doi.org/10.1111/nph.17946.

Tiwari, M., Kumar, R., Min, D., and Jagadish, S.V.K. (2022). Genetic and molecular mechanisms underlying root architecture and function under heat stress—a hidden story. Plant Cell Environ. **45**:771–788. https://doi.org/10.1111/pce.14266.

Ubeda-Tomás, S., Federici, F., Casimiro, I., Beemster, G.T.S., Bhalerao, R., Swarup, R., Doerner, P., Haseloff, J., and Bennett, M.J. (2009). Gibberellin signaling in the endodermis controls Arabidopsis root meristem size. Curr. Biol. **19**:1194–1199. https://doi.org/10.1016/j.cub.2009.06.023.

Ubogoeva, E.V., Zemlyanskaya, E.V., Xu, J., and Mironova, V. (2021). Mechanisms of stress response in the root stem cell niche. J. Exp. Bot. **72**:6746–6754. https://doi.org/10.1093/jxb/erab274.

Valdés-López, O., Batek, J., Gomez-Hernandez, N., Nguyen, C.T., Isidra-Arellano, M.C., Zhang, N., Joshi, T., Xu, D., Hixson, K.K., Weitz, K.K., et al. (2016). Soybean roots grown under heat stress show global changes in their transcriptional and proteomic profiles. Front. Plant Sci. **7**. https://doi.org/10.3389/fpls.2016.00517.

van den Berg, C., Willemsen, V., Hendriks, G., Weisbeek, P., and Scheres, B. (1997). Short-range control of cell differentiation in the Arabidopsis root meristem. Nature **390**:287–289. https://doi.org/10.1038/36856.

van der Voort, M., Kempenaar, M., van Driel, M., Raaijmakers, J.M., and Mendes, R. (2016). Impact of soil heat on reassembly of bacterial communities in the rhizosphere microbiome and plant disease suppression. Ecol. Lett. **19**:375–382. https://doi.org/10.1111/ele.12567.

Vogel, C.M., Potthoff, D.B., Schäfer, M., Barandun, N., and Vorholt, J.A. (2021). Protective role of the Arabidopsis leaf microbiota against a bacterial pathogen. Nat. Microbiol. **6**:1537–1548. https://doi.org/10.1038/s41564-021-00997-7.

Wang, R., Zhang, Y., Kieffer, M., Yu, H., Kepinski, S., and Estelle, M. (2016). HSP90 regulates temperature-dependent seedling growth in Arabidopsis by stabilizing the auxin co-receptor F-box protein TIR1. Nat. Commun. **7**:10269. https://doi.org/10.1038/ncomms10269.

Whitt, L., Ricachenevsky, F.K., Ziegler, G.Z., Clemens, S., Walker, E., Maathuis, F.J.M., Kear, P., and Baxter, I. (2020). A curated list of genes that affect the plant ionome. Plant Direct **4**:e00272. https://doi.org/10.1002/pld3.272.

Xu, J., Belanger, F., and Huang, B. (2008). Differential gene expression in shoots and roots under heat stress for a geothermal and non-thermal Agrostis grass species contrasting in heat tolerance. Environ. Exp. Bot. **63**:240–247. https://doi.org/10.1016/j.envexpbot.2007.11.011.

Yang, X., Dong, G., Palaniappan, K., Mi, G., and Baskin, T.I. (2017). Temperature-compensated cell production rate and elongation zone length in the root of Arabidopsis thaliana. Plant Cell Environ. **40**:264–276. https://doi.org/10.1111/pce.12855.

Zhang, H., Wang, E., Zhou, D., Luo, Z., and Zhang, Z. (2016). Rising soil temperature in China and its potential ecological impact. Sci. Rep. **6**:35530. https://doi.org/10.1038/srep35530.

Zhang, N., Belsterling, B., Raszewski, J., and Tonsor, S.J. (2015). Natural populations of Arabidopsis thaliana differ in seedling responses to high-temperature stress. AoB PLANTS **7**. https://doi.org/10.1093/aobpla/plv101.

Zhang, W., Swarup, R., Bennett, M., Schaller, G.E., and Kieber, J.J. (2013). Cytokinin induces cell division in the quiescent center of the Arabidopsis root apical meristem. Curr. Biol. **23**:1979–1989. https://doi.org/10.1016/j.cub.2013.08.008.

Zhao, J., Lu, Z., Wang, L., and Jin, B. (2021). Plant responses to heat stress: physiology, transcription, noncoding RNAs, and epigenetics. Int. J. Mol. Sci. **22**:117. https://doi.org/10.3390/ijms22010117.

Plant Communications, Volume *4*

Supplemental information

Temperature changes in the root ecosystem affect plant functionality

Mary Paz González-García, Carlos M. Conesa, Alberto Lozano-Enguita, Victoria Baca-González, Bárbara Simancas, Sara Navarro-Neila, María Sánchez-Bermúdez, Isai Salas-González, Elena Caro, Gabriel Castrillo, and Juan C. del Pozo

Temperature changes in the root ecosystem affect plant functionality

Mary Paz González-Garcia*[1,2], Carlos M. Conesa*[1], Alberto Lozano[1], Barbara Simancas[1], Sara Navarro-Neila[1], María Sánchez-Bermúdez[1], Victoria Baca-Gonzalez[1], Elena Caro[1,2], Isai Salas-González[3], Gabriel Castrillo[4] and Juan C. del Pozo[1ψ]

[1] Centro de Biotecnología y Genómica de Plantas. Universidad Politécnica de Madrid (UPM) - Instituto Nacional de Investigación y Tecnología Agraria y Alimentaria (INIA/CSIC). Campus Montegancedo 28223 Pozuelo de Alarcón (Madrid), Spain.

[2] Departamento de Biotecnología-Biología Vegetal, Escuela Técnica Superior de Ingeniería Agronómica, Alimentaria y de Biosistemas, Universidad Politécnica de Madrid (UPM), 28040 Madrid, Spain

[3] Undergraduate Program in Genomic Sciences. Center for Genomics Sciences. Universidad Nacional Autonóma de México, Av. Universidad s/n. Col. Chamilpa, 62210. Cuernavaca Morelos, México.

[4] Future Food Beacon of Excellence & School of Biosciences, University of Nottingham, Sutton Bonington, UK

Supplemental Methods

TGRooZ device

The TGRooZ device has been patented as utility model (U202230407) and was developed in collaboration with Ibercex company (https://www.inilab.es/marca/ibercex-camaras-ultracongeladores/). The TGRooZ consists of a metallic growth box that holds a cold-regulable bottom container (Supplementary Fig. 1b). The temperature differences between the bottom and the top surface of the device generates a gradient. The gradient can be regulated (extended or limited) by modulating the temperature in the cold-regulable bottom container and is measured with a digital thermometer with a metallic probe of 35 cm long. The temperature is regulated by water chiller machine (Supplementary Fig. 1c). In the top of the device, different lids can be positioned. Here we designed two model, one to hold 12x12 cm petri dishes containing agar-based medium and other to hold zip bags until 40 cm wide.

To cultivate pots containing soil, a modified TGRooZ device was engineered. Similarly, the base of the device was refrigerated by circulating cold water using a water-cooling machine at 10ºC and the rest of the pot was isolated with polyurethane foam to allow to cool the base of the pot and force a gradient from bottom to the top of the soil. Additionally, in the base of the potholder, a small hole is made to evacuate the excess of irrigation.

Soil Gradient calculation

To determine the soil gradient a 5 digital thermometer with a 30 cm metallic probe were used. The probes were penetrated into the soil every 2 cm and temperature was recorded in the natural soil (GPS´s coordinates 40.40535848787632, -3.831371201424853) in May and June 2019 at 2 pm. The humidity and pH was recorded using a soil PhMetter (sinbadlab).

To analyze the fluctuation of the soil gradient, we measured the maximum and minimum temperature during 4 consecutive days (27^{th}-30^{th} of June, 2022) in the soil indicated above. We used some maximum-minimum digital thermometers with an extensible probe that were introduced into the soil at 5 and 15 cm from the top. We recorded the max –min temperature daily

and represented in Supplemental Figure 1C as the average of three measures from 3 different thermometers.

Tomato cultivation in germination paper

Lycopersicon esculentum, variety money maker seeds, were pre-germinated in darkness in filter paper wetted with water for 4 days. Homogeneous seedlings were then transferred to the germination paper system. This system consists in a germination paper of 20 cm wide x 30 cm height (AHLSTROM MUNKSJÖ, BINZ2.383.200350) into a transparent plastic zip bag. Small apertures were made in to bag where the seedlings is settled to allow the growth of the hypocotyl and shoot, remaining the rest of the zip closed to avoid the evaporation of the medium. The germination paper is wetted with 45 ml of one fourth MS liquid medium without sucrose at pH=5.8. The germination paper-zip system is then moved to the chamber at 26ºC (26SR), 26TGRooZ using an adapted holder for the zip bag, 36ºC (36SR) or 36TGRooZ with the same adapted holder. After 7 days growing, the root system was analyzed with the GiaRoots to quantify different parameters.

Stomatal conductance and leaf temperature

Arabidopsis seedlings were germinated in half-strength MS medium (MS1/2) with vitamins plus 1% sucrose and 1% Difco Agar, 0,05% MES and pH=5.8 using the D-Root. After 7 days, they were transferred to pots containing 3 L of greenhouse substrate soil. These seedlings were grown for 3 weeks at 22ºC in shoot and root; (22SR), 32ºC in root and shoot, (32SR) or 32TGRooZ (32ºC in shoot and gradient from 32 to 24ºC in the root) and irrigated with 100 ml of sterile water twice a week. The water content was recorded using a Teros 10 probe (Meter group) and the Zentra Z6 datalogger every 8 hours for an entire period of 3 weeks to verify that the water content was not limited in the experiment.

Stomatal conductance (mmol m−2 s−1) was measured using a leaf porometer (model SC-1, Decagon Devices, Inc., Pullman, WA, USA). Instrument calibration was done prior each set of measurements according to manufacturer's guidelines. Two leaves from the same position in each

plants was measured in three different replicates and temperature conditions. Limiting the number of leaves on which to measure stomatal conductance was done to minimize the variability in stomatal conductance due to meteorological factors. The total number of leaves used in the experiment was always greater than eighteen. Soil water content was measured to uncouple with stomatal conductance.

Thermal pictures were taken with a FLIR-E96 camera and leaf temperature was quantified using the FLIR research studio (https://www.flir.es/products/flir-thermal-studio-suite). We quantify more than 30 leaves per temperature treatment from 3 different experiments.

Gene network generation

A gene regulatory network is a collection of molecular regulators that interact with each other and with other substances in the cell to govern the gene expression levels of mRNA and proteins, which, in turn, determine the function of the cell. Gene Network Inference with Ensemble of trees (GENIE3), a GRN inference method based on variable selection with ensembles of regression trees. It produces a directed graph of regulatory interactions and naturally allows for the presence of feedback loops in the network. During DESeq2 analysis, the normalized counts were obtained for both root and shoot samples, using the median of ratios method. These normalized counts show a new value of the count divided by the total number of observations. For each comparison, 32SR_vs_22SR, TGRZ_vs_22SR and TGRZ_vs_32SR, it is created a new *.csv file, containing the normalized counts for each gene within the samples belonging to the temperature conditions required for each comparison. These files will be the source to create the expression matrix using the by GENIE3 software, where each row belongs to a gene and every column belongs to a sample at a certain temperature condition. Each entry in the matrix represents the expression level of a particular gene in a given sample. All the genes in every condition must have unique reads assigned to that gene in that sample in order to be processed by GENIE3. In order to add more biological meaning to the GRNs, additional information like identifying transcription factors among the whole list of genes can be given. This additional information would provide more reliability to the network and robustness to the interaction between genes. With the expression

matrix and the extra information, GENIE3 can generate the weight matrix for each comparison. The algorithm outputs a matrix containing the weights of the putative regulatory links, with higher weights corresponding to more likely regulatory links. The next step is to generate the linklists for each comparison, containing the ranking of links. This link list gets the weight matrix as the input and creates all the interactions between genes existing among the data. These linklist contain rows corresponding to regulatory links, whose first column shows the regulator (i), the second shows the target gene (j) and the last columns shows the weight (im) of the connection between genes (i and j). Since the algoritm has some randomness within, the same values in the same linklist executed at different times, will vary slightly. This linklist is a large file with as many rows as interactions set earlier. Usually there is no need to get all the links between genes, and some of the interactions might have a value of 0, so it is possible to get only the most regulatory links with or to filter the matrix adding a minimum weight threshold. This threshold is recommended to be set to erase all the links whose value is equal to 0 or close to 0.

Microbiota analyses

For the analyses of microbiota abundances, tomato seeds were germinated at 22ºC during 1 week in sterile vermiculite. Afterwards, seedlings were transferred to pots (1 per pot) filled with 3 liter of natural soil obtained from coordinates 40°24'21.6"N 3°49'58.1"W that were mixed with 1 part of clean river sand. These plants were cultivated for 3 weeks at three different temperatures 22ºC (22ºC shoot and root; 22SR), 36ºC (36ºC in root and shoot, 36SR) and 36TGRZ (36ºC in shoot and gradient from 36 to 20ºC in root) and irrigated with 150 ml of sterile water twice a week. We took 6 samples of the initial soil and maintained them at -20ºC. After 3 weeks, we took 6 samples of soil corresponding to rhizosphere and 6 samples of roots that were extensively washed to eliminate soil/microorganism traces) and freeze to -20ºC. Soil and roots were taken from the same area in the pot, corresponding to an intermedium part of the root system.

After collection, samples were sent for molecular analysis to Biome Makers laboratory (https://biomemakers.com/) in Sacramento, US. DNA extraction was performed with the DNeasy PowerLyzer PowerSoil Kit from Qiagen. To characterize bacterial communities associated with

bulk soils, rhizosphere and endophytes, the 16S rRNA were selected. Libraries were prepared following the two-step PCR Illumina protocol using custom primers amplifying the 16S rRNA V4 region as described in[1]. Sequencing was conducted in an Illumina MiSeq instrument using pair-end sequencing (2x300bp).

16S rRNA amplicon sequence analysis

Briefly, raw amplicon sequences were quality filtered using fastp and then merged using pear with default parameters. The resulting high-quality filtered sequences were then denoised and collapsed into amplicon sequence variants (ASVs) using DADA2 v.1.10.1[2]. Representative ASVs sequences were taxonomically classified with the mothur naive bayes classifier trained on the SILVA 132 database[3]. We filtered ASVs that were assigned to chloroplast, mitochondria, oomycete, archaea or did not have a known kingdom assignment. After the filtering of low quality ASVs, we created rarefied and relative abundance tables using a threshold of depth of 10,000 reads per sample. The resulting abundance tables were processed and analyzed with functions from the ohchibi package (https://github.com/isaisg/ohchibi).

To compare alpha diversity across conditions and fractions, we calculated the Shannon diversity and Richness indexes using the diversity function from the vegan package v2.5-5[4]. We used ANOVA to test for differences in alpha diversity between conditions across fractions. Beta diversity analyses (Principal coordinate analysis) was based on Bray-Curtis dissimilarity matrixes calculated from the abundance table. To compute the variance explained by the Fraction effect and Temperature treatments, we performed PERMANOVA using the function adonis from the vegan package v2.5-5[4]. Bar graphs showing raw and average relative abundance of phylums across conditions was computed using the chibi.phylogram function from the ohchibi R package. We used the R package DESeq2 v.1.24.0[5] to compute the intra-fraction (Intra rhizosphere, intra root) specific enrichment profiles across the three temperature conditions. For each taxonomic unit of the following taxonomic levels, Phylum, Class, Order, Family, Genus, and ASV, we

estimated their abundance differences in each of the three temperature conditions, using a generalized linear model (GLM) with the following design:

Abundance ~ Temperature condition

Within each fraction (rhizoshphere and root), we performed the all vs all contrasts between temperature conditions (3 possible contrasts in total) and kept taxonomic units with a False Discovery Rate (FDR) p-value < 0.05. We visualized the results of the contrasts using a heatmap, in which we showed the enrichment patterns (log2 fold change) of all statistically significant taxonomic units across the three contrasts using ggplot2 v.3.2.1 R package [6]

Analysis of leaf mineral elemental profile (ionome)

The elemental profiles of leaves were measured using Inductively Coupled Plasma Mass Spectrometry (ICP-MS). The leaf material was collected and washed three times with 18.2 MΩcm Milli-Q water (Merck Millipore). The samples were placed in weighted Pyrex digestion tubes and dried at 88 ºC for 20-h. After cooling, leaf samples were weighted on Mettler five-decimal analytical scale, and 1-3 mL (depending on the sample dry weight) of the concentrated trace metal grade nitric acid Primar Plus (Fisher Chemicals) was added to each tube. Prior to the digestion, 20 µg/L of Indium (In) was added to the nitric acid as an internal standard to assess putative errors in the dilution process, variations in sample introduction and plasma stability in the ICP-MS instrument. The samples were then digested in DigiPREP MS dry block heaters (SCP Science; QMX Laboratories) for 4-h at 115 ˚C. After cooling down, the digests were diluted to 10-30 mL (depending on the volume of the nitric acid added) with 18.2 MΩcm Milli-Q Direct water and elemental analysis was performed using an ICP-MS, PerkinElmer NexION 2000 equipped with Elemental Scientific Inc 4DXX FAST Dual Rinse autosampler, FAST valve and peristaltic pump. The instrument was fitted with a PFA-ST3 MicroFlow nebulizer, baffled cyclonic C3 high sensitivity glass spray chamber cooled to 2 ºC with PC3X Peltier heated/cooled inlet system, 2.0 mm i.d. quartz injector torch and a set of nickel cones. Twenty-four elements were monitored including following stable isotopes: ^{7}Li, ^{11}B, ^{23}Na, ^{24}Mg, ^{31}P, ^{34}S, ^{39}K, ^{43}Ca, ^{48}Ti, ^{52}Cr, ^{55}Mn, ^{56}Fe,

^{59}Co, ^{60}Ni, ^{63}Cu, ^{66}Zn, ^{75}As, ^{82}Se, ^{85}Rb, ^{88}Sr, ^{98}Mo, ^{111}Cd, ^{208}Pb and ^{115}In. Helium was used as a collision gas in Kinetic Energy Discrimination mode (KED) at a flow rate of 4.5 mL/min while measuring Na, Mg, P, S, K, Ca, Ti, Cr, Mn, Fe, Ni, Cu, Zn, As, Se and Pb to exclude possible polyatomic interferences.

The remaining elements were measured in the standard mode. The instrument Syngistix™ software for ICP-MS v.2.3 (Perkin Elmer) automatically corrected any isobaric interferences. The ICP-MS measurements were performed in peak hopping scan mode with dwell times ranging from 25 to 50 ms depending on the element, 20 sweeps per reading and three replicates. The ICP-MS conditions were as follow: RF power – 1600 Watts, auxiliary gas flow rate 1.20 L/min. Torch alignment, nebuliser gas flow and quadrupole ion deflector (QID) voltages (in standard and KED mode) were optimized before analysis for highest intensities and lowest interferences (oxides and doubly charged ions levels lower than 2.5 %) with NexION Setup Solution containing 1 µg/L of Be, Ce, Fe, ln, Li, Mg, Pb and U in 1 % nitric acid using a standard built-in software procedure. To correct for variation between and within ICP-MS analysis runs, liquid reference material was prepared using pooled digested samples and run after the instrument calibration and then after every nine samples in all ICP-MS sample sets. Equipment calibration was performed at the beginning of each analytical run using seven multi-element calibration standards (containing 2 µg/L In internal standard) prepared by diluting 1000 mg/L single element standards solutions (Inorganic Ventures; Essex Scientific Laboratory Supplies Ltd) with 10 % nitric acid. As a calibration blank, 10 % nitric acid containing 2 µg/L In internal standard was used, and it was run throughout the analysis. Sample concentrations were calculated using the external calibration method within the instrument software. Further data processing, including calculation of final elements concentrations, was performed in Microsoft Excel.

Ionome analysis

We created a matrix (samples x ion) in which each cell was filled with the calculated element concentration in a given sample. Afterwards, we applied a *z*-score transformation of each

individual ion across the samples in the matrix. We compared the concentration of each ion across the three temperature treatments by applying a linear model with the following design:

$$\text{Ion Concentration} \sim \text{Temperature Condition}$$

After fitting the model, we determined statistical significant differences between conditions by performing pairwise comparisons and visualizing the results of the comparisons using the compact letter display (CLD) as implemented in the in the multcomp v.1.4-12 R package.

The abundance profiles of each ion across temperature conditions was visualized using a heatmap created by the ggplot2 v.3.2.1 R package [6] using the standardized (z-score) ion abundance.

References

1 Ortiz-Álvarez, R. *et al.* Emergent properties in microbiome networks reveal the anthropogenic disturbance of farming practices in vineyard soil fungal communities. *bioRxiv*, 2020.2003.2012.983650, doi:10.1101/2020.03.12.983650 (2020).

2 Callahan, B. J. *et al.* DADA2: High-resolution sample inference from Illumina amplicon data. *Nature Methods* **13**, 581-583, doi:10.1038/nmeth.3869 (2016).

3 Quast, C. *et al.* The SILVA ribosomal RNA gene database project: improved data processing and web-based tools. *Nucleic Acids Research* **41**, D590-D596, doi:10.1093/nar/gks1219 (2012).

4 Oksanen, J. *et al.* Package "vegan." Community Ecol. Package Version 2. *Package 'vegan.'Community Ecol Packag version* **2** (2013).

5 Love, M. I., Huber, W. & Anders, S. Moderated estimation of fold change and dispersion for RNA-seq data with DESeq2. *Genome Biol* **15**, 550, doi:10.1186/s13059-014-0550-8 (2014).

6 Wickham, H. Ggplot2: Elegant graphics for data analysis (2nd ed.). *Springer* International *Publishing.* (2016).

7 Huynh-Thu V, Irrthum A, Wehenkel L, Geurts P (2010). "Inferring regulatory networks from expression data using tree-based methods." PLoS ONE, 5(9), e12776. doi: 10.1371/journal.pone.0012776.

Supplemental Figures

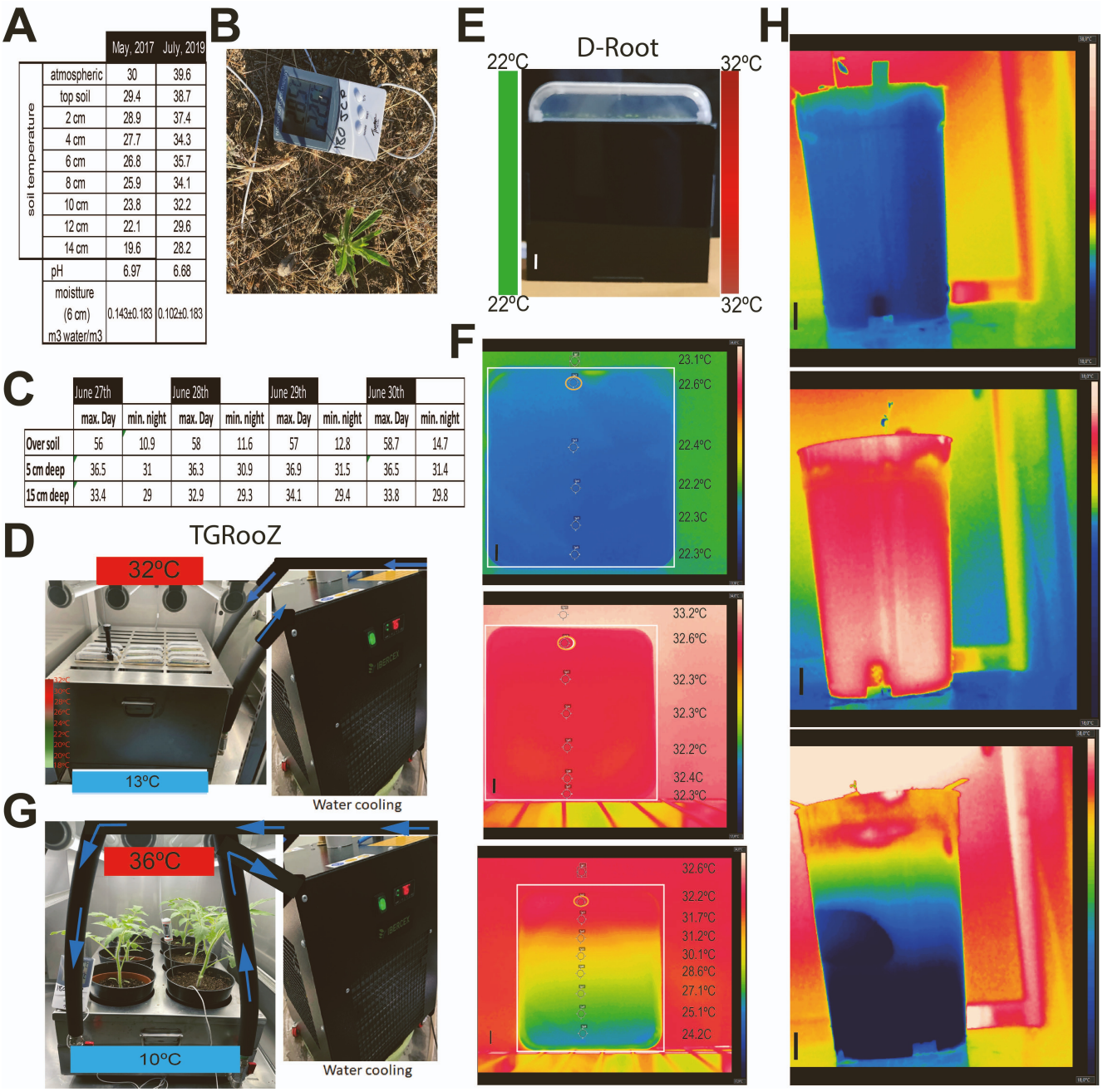

		May, 2017	July, 2019
soil temperature	atmospheric	30	39.6
	top soil	29.4	38.7
	2 cm	28.9	37.4
	4 cm	27.7	34.3
	6 cm	26.8	35.7
	8 cm	25.9	34.1
	10 cm	23.8	32.2
	12 cm	22.1	29.6
	14 cm	19.6	28.2
	pH	6.97	6.68
	moistture (6 cm) m3 water/m3	0.143±0.183	0.102±0.183

	June 27th		June 28th		June 29th		June 30th	
	max. Day	min. night	max. Day	min. night	max. Day	min. night	max. Day	min. night
Over soil	56	10.9	58	11.6	57	12.8	58.7	14.7
5 cm deep	36.5	31	36.3	30.9	36.9	31.5	36.5	31.4
15 cm deep	33.4	29	32.9	29.3	34.1	29.4	33.8	29.8

Supplemental Figure 1: TGRooZ device. (A) Temperature of the soil (GPS´s coordinates 40.40535848787632, -3.831371201424853) in May and June 2019 using a digital thermometer containing a metal probe. Measured were taken every 2 cm and the temperatures correspond to the average of 3 different measures. **(B)** Digital thermometer with an external probe to measure maxima and minima temperatures at 5 or 15 cm deep. **(C)** Maxima and minima temperatures during 4 days in natural soil (GPS´s coordinates 40.40535848787632, -3.831371201424853) between June 27th and 30th, 2022. **(D)** TGRooZ device to cultivate seedlings in 12x12 cm petri dishes containing agar-based

medium. To generate a temperature gradient in the root zone the base of the device is refrigerated by circulating cold water at 10-13 ºC, depending on the gradient desired, using a water-cooling machine. **(E)** D-Root system to preserve the roots from direct illumination. Seedling in the D-Root were cultivated to homogeneous 22ºC (22SR) or 32ºC (32SR). Scale bar corresponds to 1 cm. **(F)** Thermal pictures of 22SR, 32SR or 32TGRooz Petri 12x12 plates Notice the temperature gradient formed in the 32TGRooZ. Circles named as SP were used to calculate the temperature in the area using the FLIR studio software. The top SP corresponds to the chamber temperature. Yellow circles indicate the position of the shoots in the plate. seedlings. Scale bars correspond to 1 cm. **(G)** Modified TGRooZ device to cultivate plants in pots containing soil. Similarly, the base of the device was refrigerated by circulating cold water using a water-cooling machine at 10ºC. Right picture corresponds to pots cultivate at high-homogeneous temperature of 36ºC (36SR). **(H)** Thermal pictures of pots cultivated at 22ºC (22SR), 36ºC (36SR) or 36TGRooZshowing the homogeneous temperature or the gradient formed. Scale bars correspond to 5 cm.

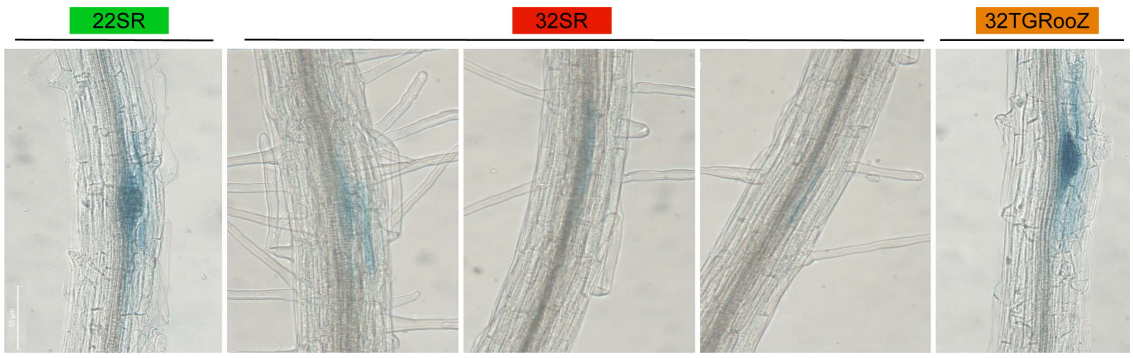

Supplemental Figure 2: High temperature blocks lateral root primordia formation. SKP2Bp::GUS seedlings were germinated at 22ºC from 4 days. Afterwards, they were transferred to 22ºC (SR22), 32ºC (SR32) or 32TGRooZ for 6 extra days. Then, these seedlings were stained for GUS activity directly on the plate to analyze the effect of high temperature after the transference point.

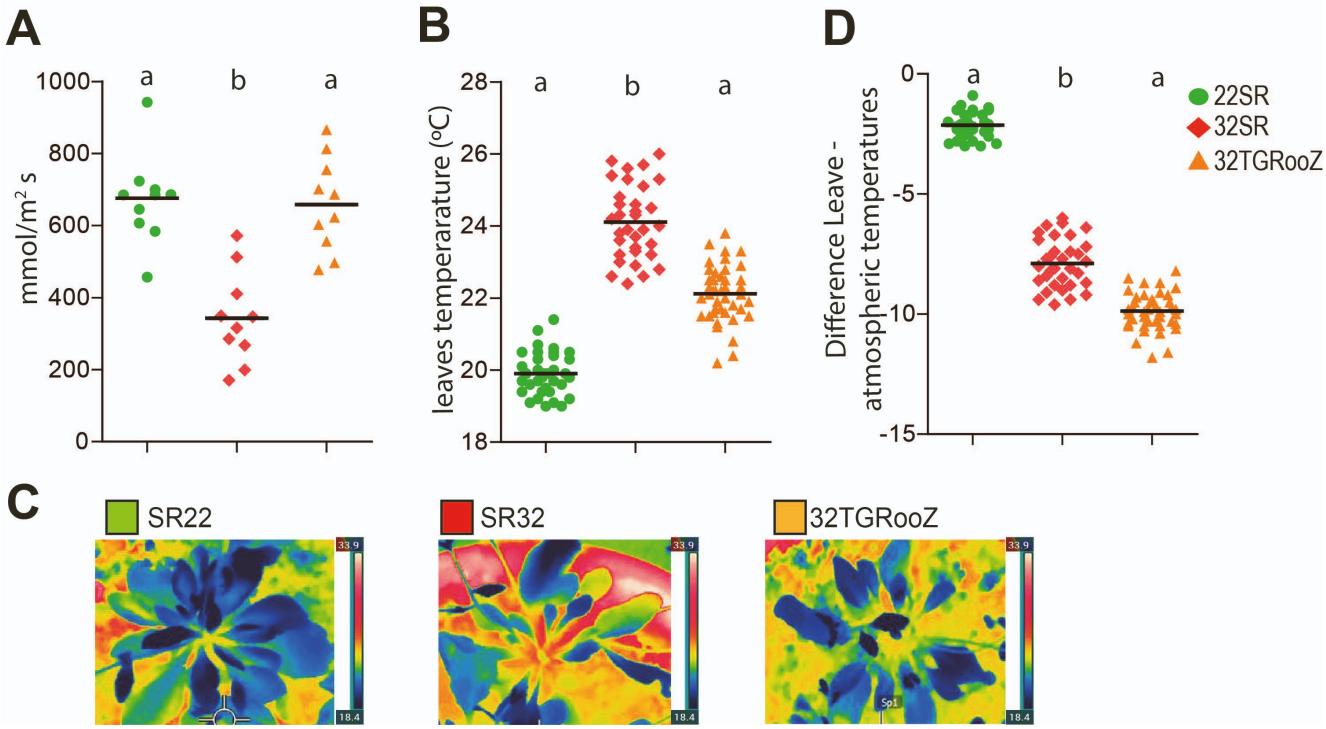

Supplemental Figure 3: Temperature in the root zone affects leave conductance and leave temperature. (A) Conductance (mol / m^2 s) of leaves of Arabidopsis plants grown in pots containing soil at 22ºC (22SR), 32ºC (32SR) or the modified 32TGRooZ for 2 weeks in the modified. n = 8. **(B)** Leaves temperature of plants grown as in the conditions explained in a. n≥33. **(C)** Representative thermal pictures of plants analyzed in b. Error bars correspond to standard deviation. **(D)** Temperature difference between atmosphere and the leaves of 22SR, 32SR or 32TGRooZ. Significance was analyzed by ANOVA and Tukey HSD post-test. $P < 0.05$. Different letters indicate significant differences.

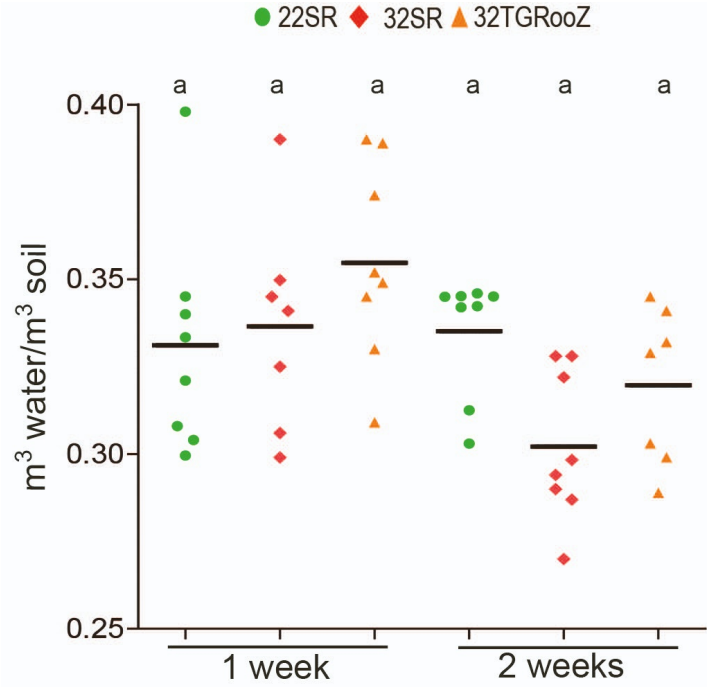

Supplemental Figure 4: Water content. Quantification of water content in the soil through all temperatures analyzed (22ºC, 22SR; 32ºC, 32SR and TGRooZ, 32TGRooZ). The graphs represent the measures taken by different probes at 1 week or 2 weeks after the Arabidopsis seedlings were transplanted to soil. We used the Teros 10 probe (Meter group) and, using the Zentra Z6 datalogger, the water content was recorded every 8 hours for an entire period of 2 weeks. Significance was analyzed by ANOVA and Tukey HSD post-test. $P < 0.05$. Different letters indicate significant differences.

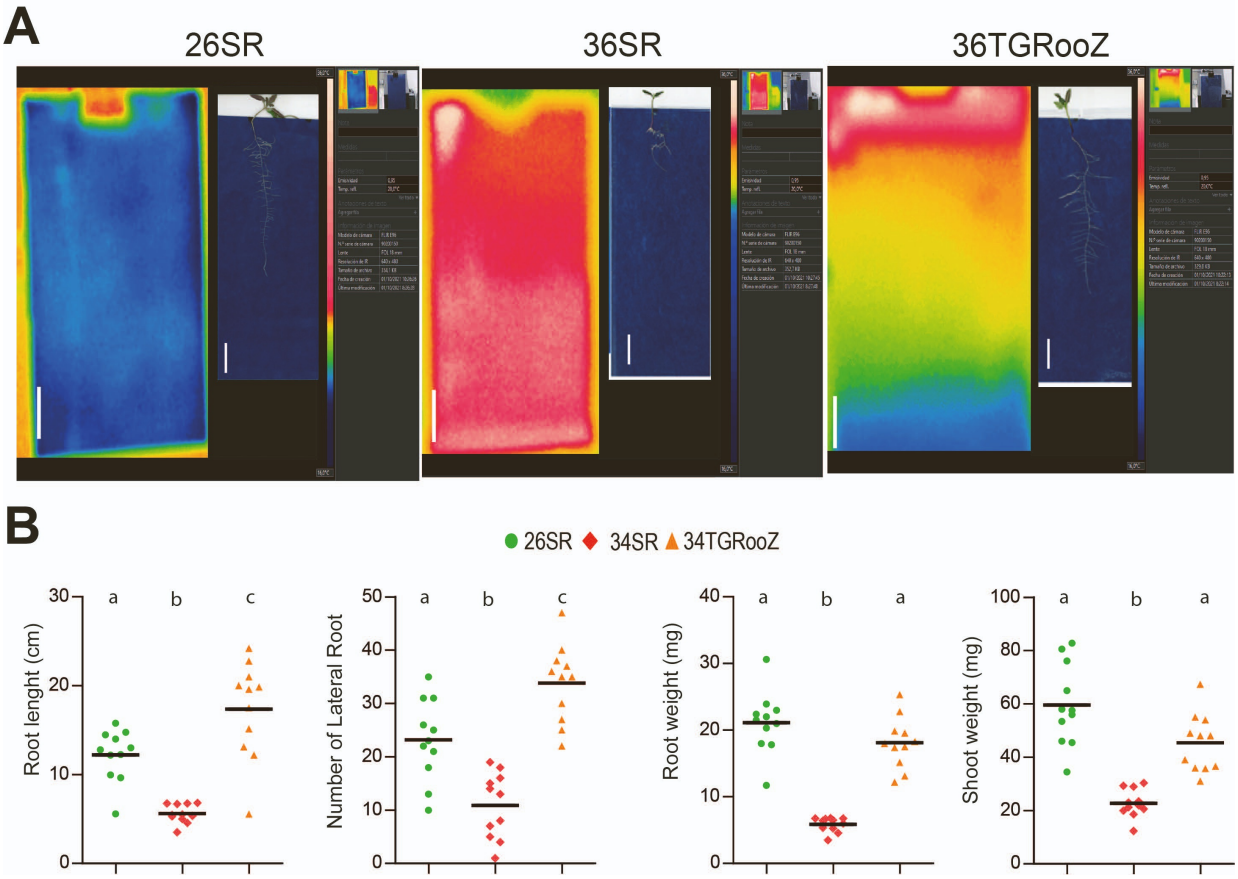

Supplemental Figure 5: Effect of TGRooZ in tomato seedlings. (A) Optical and thermal pictures, taken with a FLIRE96, of the germination paper cultivated at 26ºC, 36ºC or 36TGRooZ showing the homogeneous temperature or the gradient formed. Right photographs correspond to representative pictures of tomato seedling grown in those conditions. Tomato seeds were stratified for 4 days at 4ºC and then they were germinated in darkness for 5 days. Afterwards, seedlings were transferred to germination paper into a zip bag for 7 days. The paper was wetted with one-fourth of MS salts plus 1 mM of MES at pH=5.8. Scale bars correspond to 5 cm. **(B)** Root length, lateral root number, root and shoot fresh weight of 26SR, 36SR or 36TGRooZ tomato seedlings grown for 7 days after transplanting. Significance was analyzed by ANOVA and Tukey HSD post-test. $P < 0.05$. Different letters indicate significant differences.

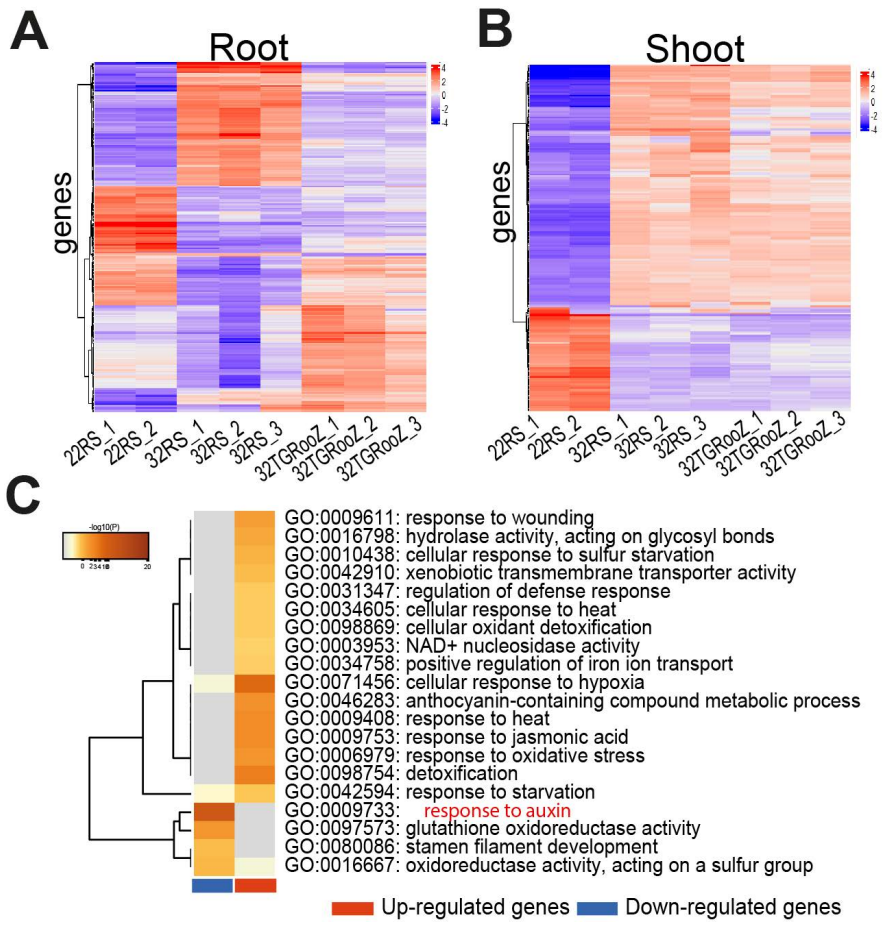

Supplemental Figure 6: Temperature gradient in the root zone modifies gene expression in the shoots under heat stress affecting the auxin response. (**A-B**) Clustering of the genes showing the highest variance in root **(A)** or shoot **(B)** samples of seedlings grown a 22RS, 32SR or 32TGRooZ. **(C)** Gene ontology heat map of shoots differentially expressed genes (DEG) from the 32SR vs 32TGRooZ (32SR_TGRooZ) comparisons. Red and blue boxes correspond to up- or down-regulated genes respectively.

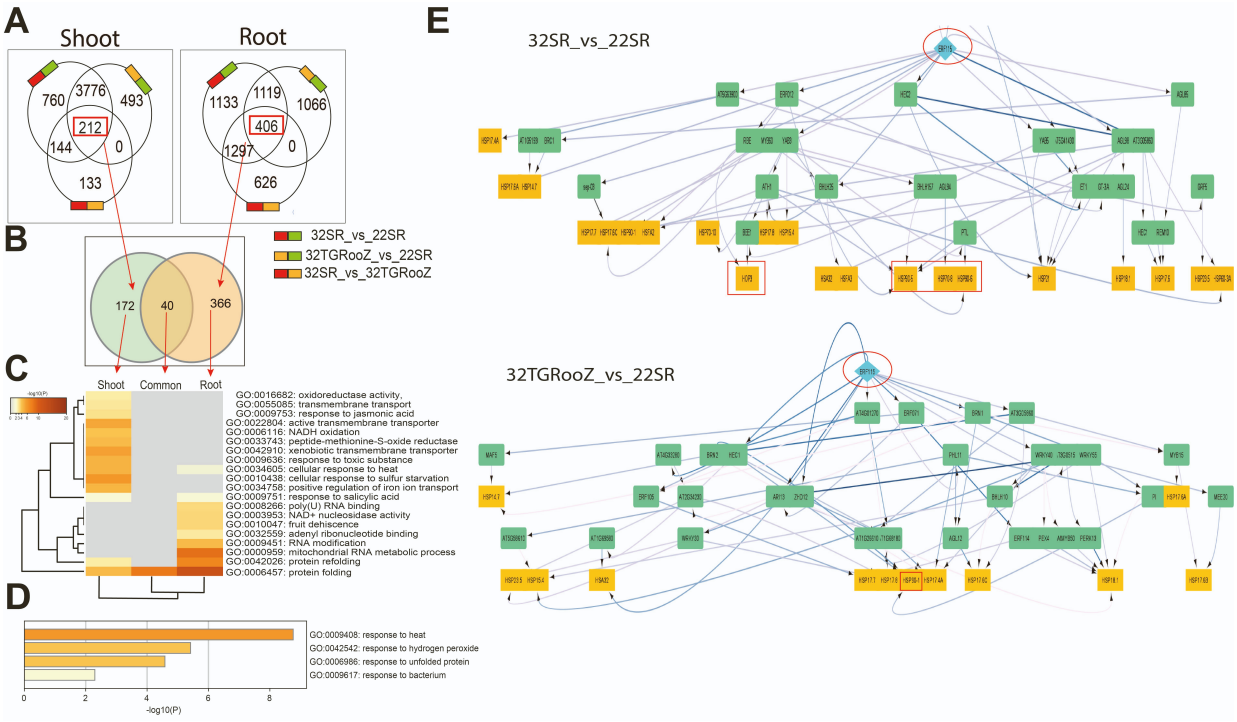

Supplemental Figure 7: Identification of genes regulated by high temperature. (**A**) Venn diagrams of genes upregulated by the effect of temperature in root and shoot in all the treatments (32SR vs 22SR, 32SR vs 32TGRooZ and 32TGRooZ vs 22SR). (**B**) Venn diagram of common upregulated genes identified in a. (**C**) Gene ontology heat map of DEG analyzed in b (shoot specific, root specific or common). (**D**) Gene ontology heat map of common DEG identified in B, analyzed in Metascape. (**E**) Gene network connecting *ERF115* transcription factor (red ellipse) with genes deregulated in the comparison between 32SR versus 22SR or 32TGRooZ versus 22SR. Red rectangles indicate HSP70 and HSP90 genes.

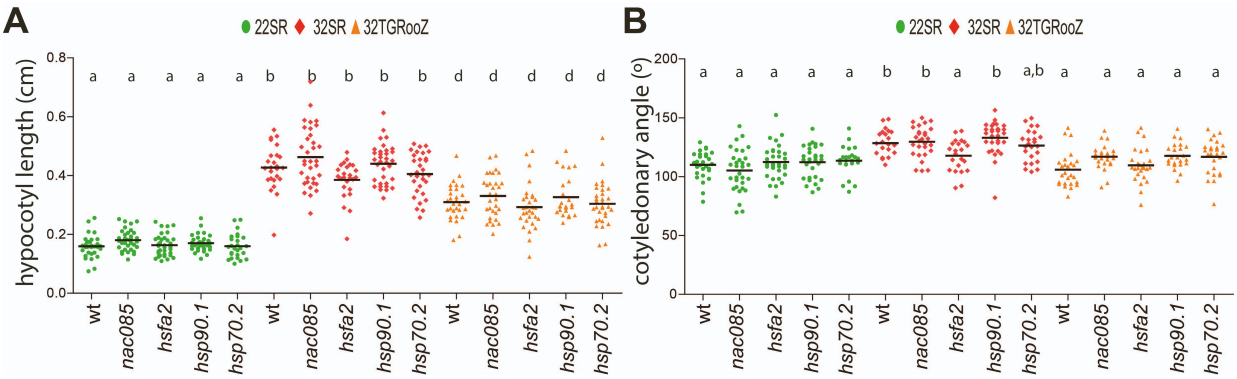

Supplemental Figure 8: Effect of high temperature and the temperature gradient in the root zone on heat response mutants. **(A)** Hypocotyl length of 22SR, 32SR or 32TGRooZ wild type (wt) and mutant seedlings. **(B)** Cotyledonary angle of 22SR, 32SR or 32TGRooZ wt and mutant seedlings. n≥24. Significance was analyzed by ANOVA and Tukey HSD post-test. Different letters indicate significant differences.

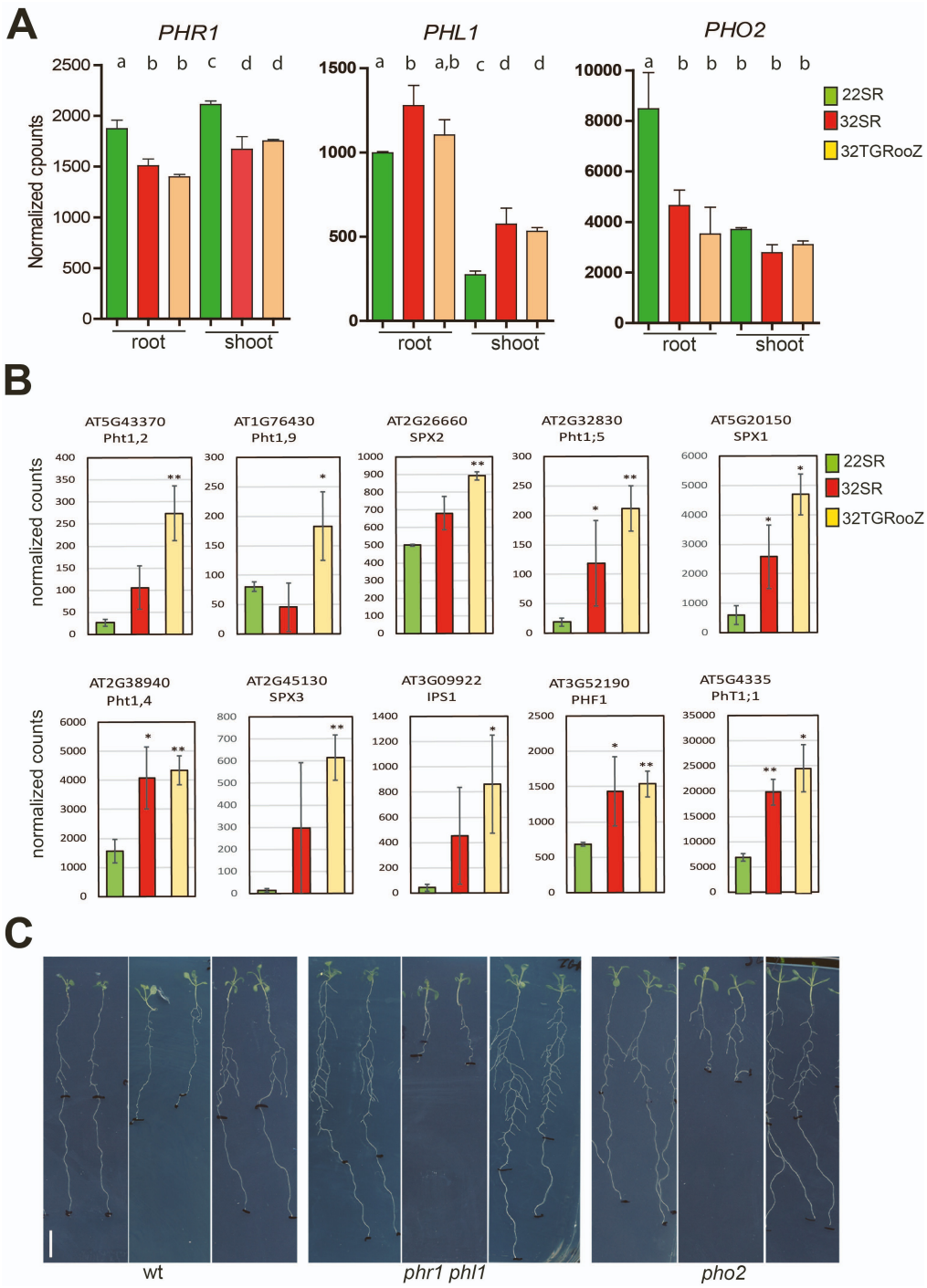

Supplemental Figure 9: Heat stress alters the expression of phosphate starvation response genes. **(A)** Effect of root temperature in the expression on *PHR1, PHL1* and *PHO2* genes. Values correspond to normalized counts from our RNAseq experiments in both shoot and root. Significance was analyzed by ANOVA and Tukey HSD post-test. **(B)** Effect of root temperature in the expression of genes involved in the Pi starvation response. Values correspond to normalized counts from our RNAseq experiments in roots. *, $P < 0.05$; **, $P < 0.01$ by T-test. **(C)** Representative pictures of wild type (wt) phr1 phl1 double mutant or pho2 mutant grown at 22ºC for 4 days and then transferred to 22ºC, 32ºC or 32TGRooZ for 6 extra days.

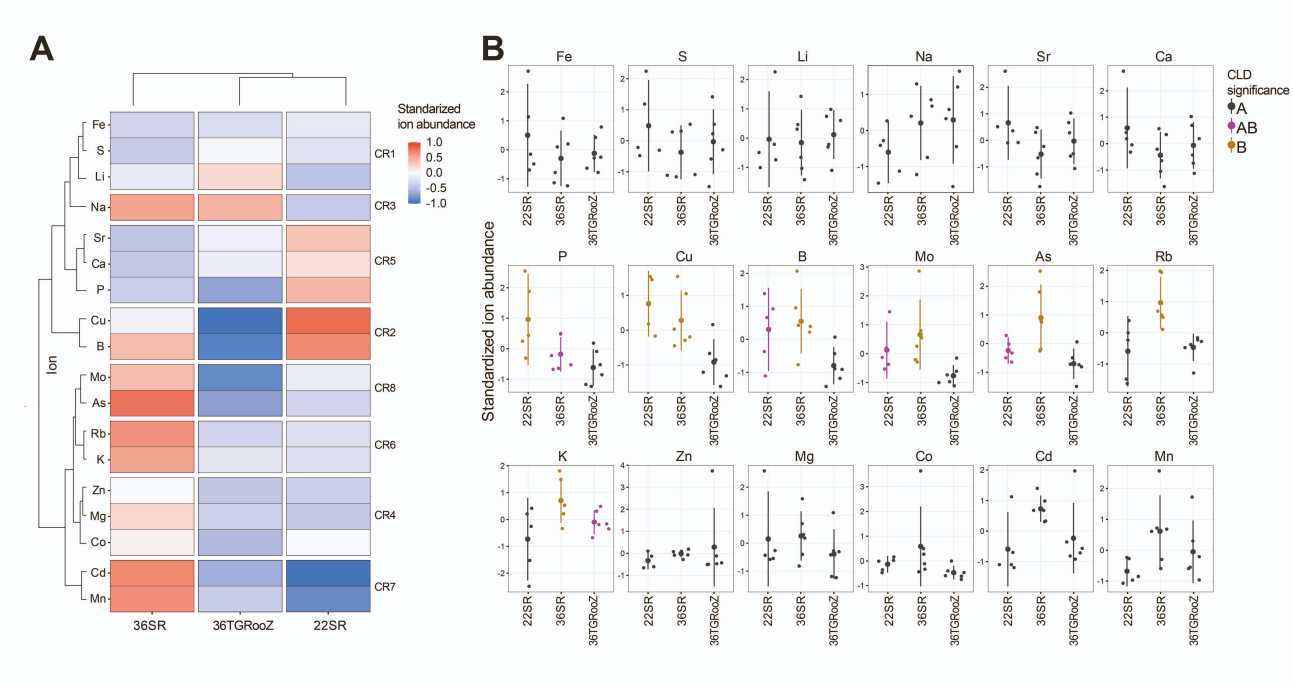

Supplemental Figure 10: High temperature in the root affects mineral nutrient accumulation in tomato leaves. **(A)** Clustered heatmap showing the standardized mineral nutrient concentration in leaves of tomato plants grown at 22ºC (22SR), 36ºC (36SR) or 36ºC with a temperature gradient in the root zone (36TGRooZ) for 4 weeks. C letter represents different clusters. **(B)** Individual standardized mineral nutrient abundances across the temperature treatments used in A**.** Significance was determined via pairwise comparisons and the results visualised using the compact letter display (CLD).

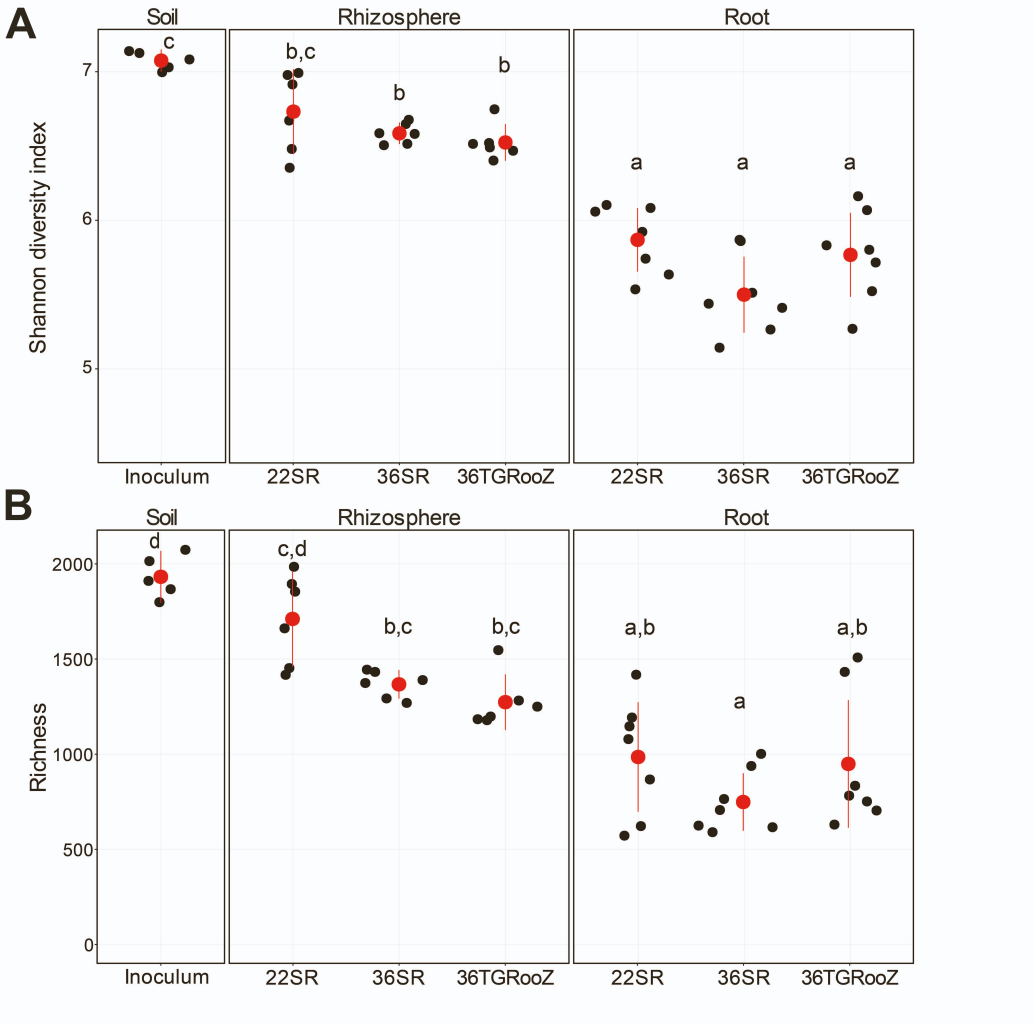

Supplemental Figure 11: Soil and rhizosphere support a higher bacterial alpha diversity as compared with roots in tomato. (A) Bacterial alpha diversity estimated using the Shannon Diversity. **(B)** Richness indexes in soil, rhizosphere, and root-associated samples of tomato plants grown at 22ºC (22SR), 36ºC (36SR) or 36TGRooZ for 4 weeks. Letters represent post hoc test results, based on a full factorial ANOVA model.

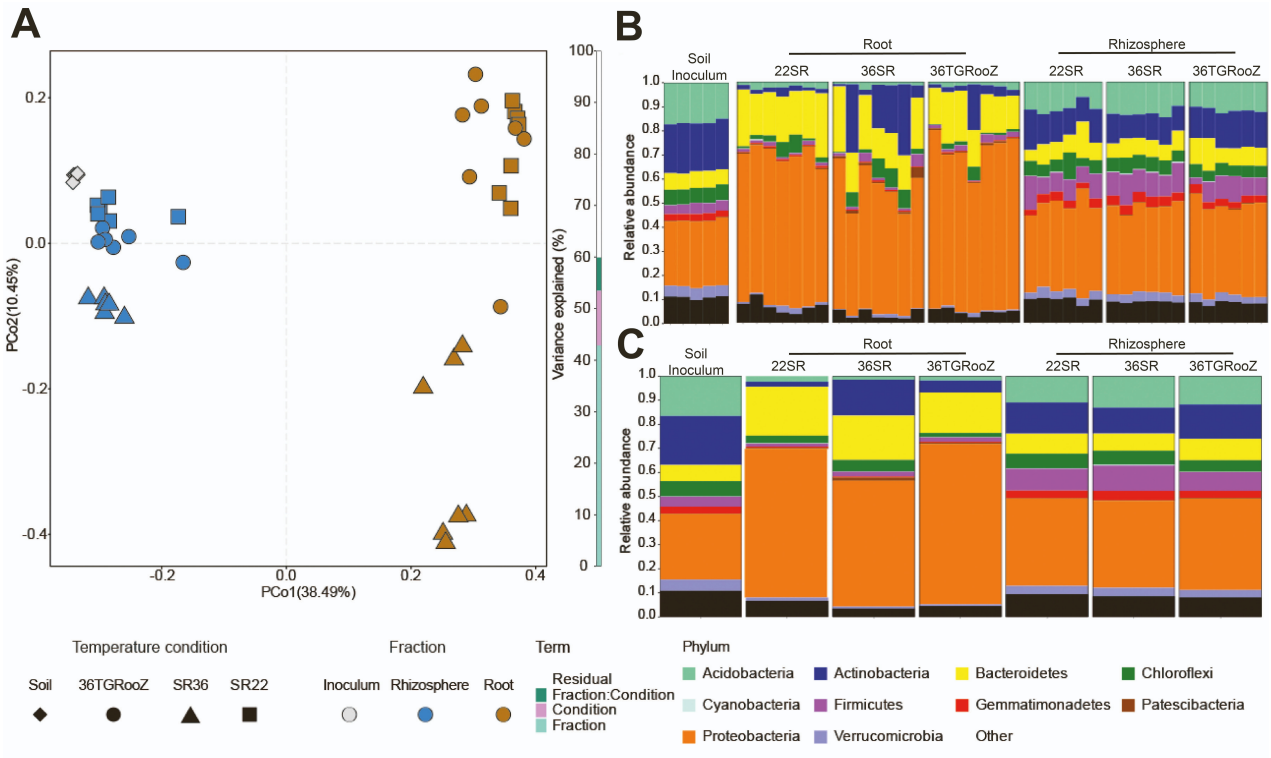

Supplemental Figure 12: Bacterial composition profiles of tomato plants exposed to different temperature treatments. (A) Principal coordinates analysis (PCo) based on Bray-Curtis dissimilarities between bacterial communities in soil, rhizosphere, and roots of tomato plants grown at 22ºC (22SR), 36ºC (36SR) or 36TGRooZ for 4 weeks. The bar graph to the right of the PCo shows the percentage of variance explained in a PERMANOVA model ($p < 0.05$). **(B,C)** Bars show individual **(B)** or Mean relative **(C)** abundance profiles of the ma.in bacterial phyla found in soil, rhizosphere, and roots of tomato plants from **A**.